

1 *Burkholderia* collagen-like protein 8, Bucl8, is a unique outer membrane component of a  
2 tetrapartite efflux pump in *Burkholderia pseudomallei* and *Burkholderia mallei*

3

4 Megan E Grund<sup>1</sup>, Soo J Choi<sup>1</sup>, Dudley H McNitt<sup>1</sup>, Mariette Barbier<sup>1</sup>, Gangqing Hu<sup>1,2,3</sup>,  
5 Paul R LaSala<sup>4</sup>, Christopher K. Cote<sup>5</sup>, Rita Berisio<sup>6</sup>, Slawomir Lukomski<sup>1,2\*</sup>

6

7 <sup>1</sup>Department of Microbiology, Immunology and Cell Biology, School of Medicine, West  
8 Virginia University, Morgantown, WV, United States of America

9 <sup>2</sup>Cancer Center, West Virginia University, Morgantown, WV, United States of America

10 <sup>3</sup>Bioinformatics Core, West Virginia University, Morgantown, WV, United States of  
11 America

12 <sup>4</sup>Department of Pathology, West Virginia University, Morgantown, WV, United States of  
13 America

14 <sup>5</sup>Bacteriology Division, The United States Army Medical Research Institute of Infectious  
15 Diseases (USAMRIID), Frederick, MD, United States of America

16 <sup>6</sup>Institute of Biostructures and Bioimaging, National Research Council, Naples, Italy

17

18

19 \*Corresponding author

20 E-mail: slukomski@hsc.wvu.edu (SL)

21

## 22 **Abstract**

23 Bacterial efflux pumps are an important pathogenicity trait because they extrude a  
24 variety of xenobiotics. Our laboratory previously identified *in silico Burkholderia*  
25 collagen-like protein 8 (Bucl8) in the Tier one select agents *Burkholderia pseudomallei*  
26 and *Burkholderia mallei*. We hypothesize that Bucl8, which contains two predicted  
27 tandem outer membrane efflux pump domains, is a component of a putative efflux  
28 pump. Unique to Bucl8, as compared to other outer membrane proteins, is the presence  
29 of an extended extracellular region containing a collagen-like (CL) domain and a non-  
30 collagenous C-terminus (Ct). Molecular modeling and circular dichroism spectroscopy  
31 with a recombinant protein, corresponding to this extracellular CL-Ct portion of Bucl8,  
32 demonstrated that it adopts a collagen triple helix, whereas functional assays screening  
33 for Bucl8 ligands identified binding to fibrinogen. Bioinformatic analysis of the *bucl8*  
34 gene locus revealed it resembles a classical efflux-pump operon. The *bucl8* gene is co-  
35 localized with downstream *fusCDE* genes encoding fusaric acid (FA) resistance, and  
36 with an upstream gene, designated as *fusR*, encoding a LysR-type transcriptional  
37 regulator. Using RT-qPCR, we defined the boundaries and transcriptional organization  
38 of the *fusR-bucl8-fusCDE* operon. We found exogenous FA induced *bucl8* transcription  
39 over 80-fold in *B. pseudomallei*, while deletion of the entire *bucl8* locus decreased the  
40 MIC of FA 4-fold in its isogenic mutant. We furthermore showed that the Bucl8 pump  
41 expressed in the heterologous *Escherichia coli* host confers FA resistance. On the  
42 contrary, the Bucl8 pump did not confer resistance to a panel of clinically-relevant  
43 antimicrobials in *Burkholderia* and *E. coli*. We finally demonstrated that deletion of the  
44 *bucl8*-locus drastically affects the growth of the mutant in L-broth. We determined that

45 Bucl8 is a component of a novel tetrapartite efflux pump, which confers FA resistance,  
46 fibrinogen binding, and optimal growth.

47

## 48 **Author Summary**

49 *Burkholderia pseudomallei* and *Burkholderia mallei* are highly infectious and  
50 multidrug resistant bacteria that are classified by the National Institute of Allergy and  
51 Infectious Diseases as Tier one select agents partly due to the intrinsic multidrug  
52 resistance associated with expression of the efflux pumps. To date, only few efflux  
53 pumps predicted in *Burkholderia* spp. have been studied in detail. In the current study  
54 we introduce Bucl8, an outer membrane component of an unreported putative efflux  
55 pump with a unique extended extracellular portion that forms a collagen triple helix and  
56 binds fibrinogen. We demonstrate Bucl8's role in fusaric acid resistance by defining its  
57 operon via bioinformatic and transcriptional analyses, as well as by employing loss-of-  
58 function and gain-of-function genetic approaches. Our studies also implicate the Bucl8-  
59 associated pump in metabolic and physiologic homeostasis. Understanding how Bucl8  
60 efflux pump contributes to *Burkholderia* pathology will foster development of pump  
61 inhibitors targeting transport mechanism or identifying potential surface-exposed  
62 vaccine targets.

## 63 Introduction

64 *Burkholderia pseudomallei* and *Burkholderia mallei* are Gram-negative bacteria that  
65 are the etiological agents of melioidosis and glanders, respectively [1]. Both pathogens  
66 are highly virulent and easily aerosolized, therefore they are classified as Tier one  
67 select agents by both the U.S. Department of Health and Human Services and the U.S.  
68 Department of Agriculture. In addition to being a biodefense concern, the bacteria are  
69 highly resistant to antibiotics and currently there is no licensed vaccine for either  
70 pathogen. Increasing global investigation into melioidosis has indicated that the disease  
71 may be more widespread than originally reported [2], and it has one of the highest  
72 disability-adjusted life years (DALY) of neglected tropical diseases at 4.6 million [3].

73 *B. pseudomallei* is a soil saprophyte that can infect humans, resulting in symptoms  
74 ranging from localized infections, including swelling or ulcerations, to systemic infections  
75 that can lead to septic shock [4]. Treatment includes an extensive two-part  
76 chemotherapeutic regimen, most commonly using ceftazidime intravenously and then  
77 following it with an oral antibiotic eradication therapy of co-trimoxazole and doxycycline  
78 [5]. *B. mallei* is a clonal derivative of *B. pseudomallei* that has undergone significant  
79 genomic reduction and rearrangement. This genomic evolution is attributed to the  
80 species transition from being a soil saprophyte to an obligate host pathogen, selecting  
81 for genes advantageous for host-survival [6]. Glanders primarily affects equines, but can  
82 infect other livestock such as donkeys and goats. Although uncommon in humans, this  
83 zoonotic disease is often fatal if left untreated [4]. Symptoms typically affect the  
84 pulmonary system, including pneumonia and lung abscess, but may also present as  
85 cutaneous ulceration following direct inoculation.

86 Several classes of efflux pumps are expressed in multidrug resistant Gram-negative  
87 bacteria, such as *Pseudomonas aeruginosa*, *Acinetobacter baumannii*, and  
88 *Burkholderia spp.*, and are at least partly responsible for their intrinsic antimicrobial  
89 resistance, including resistance-nodulation division (RND) efflux pumps [7].  
90 *Burkholderia* are notorious for being resistant to an array of antibiotics, such as  $\beta$ -  
91 lactams, aminoglycosides, tetracyclines, fluoroquinolones, macrolides, polymyxins, and  
92 trimethoprim [8], resulting in serious infections that are hard to treat. Bioinformatic  
93 analyses of the *B. pseudomallei* genomes have identified at least ten RND efflux pumps  
94 [9], although only three systems were characterized in more detail, e.g., AmrAB-OprA,  
95 BpeAB-OprB, and BpeEF-OprC [10]; this gap in knowledge underscores a need for  
96 more studies of drug efflux pumps in *Burkholderia* [11]. Importantly, a large body of  
97 evidence indicates that efflux pumps also contribute to resistance to a variety of host-  
98 defense molecules, biofilm formation, regulation of quorum sensing and balanced  
99 metabolism, and overall pathogenesis [12], which further accentuate the importance of  
100 the efflux systems in bacteria.

101 Our previous studies have identified 13 novel *Burkholderia* collagen-like (CL)  
102 proteins (Bucl) containing collagen-like Gly-Xaa-Yaa or GXY repeats, as well as non-  
103 collagen domains, some of which had predicted functions [13]. Specifically, Bucl8 was  
104 predicted to be an outer membrane protein, containing tandem efflux pump OEP  
105 domains. Of the *Burkholderia* species tested, Bucl8 was present only in *B. pseudomallei*  
106 and *B. mallei*, although a homologous DNA sequence is present in *B. thailandensis*.  
107 Unique to Bucl8, as compared to typical outer membrane proteins, is an extended  
108 extracellular portion of unknown function that contains a presumed collagen-like

109 domain, followed by a non-collagen C-terminal region. In addition, the collagen domain,  
110 which is broadly characterized as a stretch of repeating GXY motifs [14], in Bucl8 is  
111 composed of an uncommon repeating (Gly-Ala-Ser or GAS)<sub>n</sub> collagen-like sequence.

112 Here, our objectives are to characterize the structure and function of the Bucl8-CL  
113 domain, define the *bucI8* locus, and identify substrates and potential function(s) of the  
114 putative Bucl8-associated efflux pump. We demonstrate that the collagen-like domain  
115 indeed adopts the characteristic collagen triple-helical structure. In addition, the  
116 recombinant extracellular portion of Bucl8 can bind to fibrinogen. We find that Bucl8 is  
117 the outer membrane component of an efflux pump responsible for fusaric acid (FA)  
118 resistance, a potent mycotoxin produced by *Fusarium* species that cohabitate the soil  
119 environment with *Burkholderia* [15, 16]. We further identify *bucI8*-associated genes  
120 encoding putative Bucl8-efflux-pump components. Transcripts of the *bucI8*-operon were  
121 upregulated in *B. pseudomallei* and *B. mallei* by exogenous FA, as well as by FA-  
122 derivative pHBA, which is involved in regulation of balanced metabolism in *E. coli*. FA  
123 resistance was diminished in a *B. pseudomallei* isogenic deletion mutant without the  
124 *bucI8* locus and could also be transferred to a FA-sensitive *E. coli* strain. Lastly, we  
125 found that the mutant grew at a significantly reduced rate, suggesting that under  
126 laboratory conditions the pump is important for the cell's physiology. Here, we describe  
127 a previously unreported efflux pump with unique structure and functional implications in  
128 the biology of *B. pseudomallei* and *B. mallei* species.

## 129 **Materials and Methods**

### 130 **Bacterial strains and growth**

131 Two BSL2 *Burkholderia* strains exempt from the Select Agents list were used in this  
 132 study: (i) *B. pseudomallei* strain Bp82 is an avirulent  $\Delta purM$  mutant of strain 1026b [17],  
 133 which was obtained from Christopher Cote (US AMRIID, Frederick, MD) and (ii) *B.*  
 134 *mallei* CLH001  $\Delta tonB\Delta hcp1$  mutant originates from the strain Bm ATCC23344 [18],  
 135 which was obtained from Alfredo Torres (UTMB, Galveston, TX) (**Table 1**). Strain Bp82  
 136 was routinely grown in Luria broth-Miller (LBM) with shaking at 37°C and on Luria agar  
 137 (LA) solid medium at 37°C. Strain CLH001 was grown under the same conditions, but  
 138 the broth medium was supplemented with 4% glycerol. *E. coli* strains JM109 (Promega)  
 139 and S17-1 $\lambda$ pir/pLFX (*E. coli* Genetic Stock Center, Yale University) were cultured in  
 140 LBM media and on LA. Antimicrobials were used in selective media and in  
 141 susceptibility/ resistance assays, as described in the methods below.

142 **Table 1. Bacterial strains and plasmids**

Strains and Plasmids		Description/ Characteristics	Source
<i>B. pseudomallei</i>	Bp 1026b (genomic DNA)	Blood culture from 29-year old female rice farmer with diabetes mellitus, Northeast Thailand, Sappasithiprasong hospital; 1993	BEI Resources
	Bp K96243 (genomic DNA)	Female diabetic patient- Khon Kaen hospital, Northeast Thailand; 1996	BEI Resources
	Bp82	Attenuated 1026b strain with a partial deletion of the <i>purM</i> gene resulting in adenine and thiamine auxotrophy	USAMRIID, Frederick, MD
	Bp82 $\Delta bucl8$ - <i>fusE</i>	Bucl8-pump deletion mutant	This study
<i>B. mallei</i>	CLH001	Attenuated Bm ATCC23344 mutant with genes <i>tonB</i> (iron acquisition) and <i>hcp1</i> (type 6 secretory system structural protein) deleted	UTMB, Galveston, TX
<i>E. coli</i>	JM109	Host strain; $\Delta endA1$ , $\Delta recA1$ , $\Delta lacZ$ gene	Promega
	JM109::525	JM109 with pSL525 plasmid containing the Bucl8-pump locus from Bp 1026b/Bp82	This study
	JM109::529	JM109 with pSL529 plasmid containing the Bucl8-pump locus from Bp K96243	This study



	S17-1 $\lambda$ pir/pLFX	Mobilization host	<i>E. coli</i> Genetic Stock Center, Yale University
Plasmids	pQE-30	<i>E. coli</i> expression vector for proteins with N-terminal 6xHis-tag; T5 promoter; ampicillin resistance	Qiagen
	pUC18T-mini-Tn7T-Tp	Mobilizable TpR mini-Tn7 vector; trimethoprim and ampicillin resistance	[19]
	pMo130	Mobilizable <i>E. coli</i> vector suicide in <i>Burkholderia</i>	[20]
	pSL520	pQE-30-based plasmid for expression of rBucl8-Ct protein	This study
	pSL521	pQE-30-based plasmid for expression of rBucl8-CL-Ct protein	This study
	pSL522	pMo130-based plasmid with <i>fusR</i> for generating chromosomal deletion of Bucl8-pump.	This study
	pSL524	pMo130-based plasmid with <i>fusR</i> and <i>tar</i> for generating chromosomal deletion of Bucl8-pump	This study
	pSL525	pUC18T-mini-Tn7T-Tp based plasmid with Bucl8-pump locus of Bp 1026b/Bp82	This study
	pSL529	pUC18T-mini-Tn7T-Tp based plasmid with Bucl8-pump locus of Bp K96243	This study

143

## 144 **Bioinformatic analyses of the *bucl8* locus**

### 145 ***Annotation of transcriptional and translational signals***

146 The promoter regions of *fusR* and *bucl8* were defined by combining public  
 147 transcriptome data and computational prediction. Briefly, strand-specific RNA-Seq data  
 148 of *B. pseudomallei* [21] was downloaded from National Center for Biotechnology  
 149 Information (NCBI) Sequence Read Archive (SRA) under BioProject accession  
 150 PRJNA398168. The RNA-Seq read distribution across the genome was visualized by  
 151 the UCSC genome browser [22], which includes a reference strain for 1106a. The  
 152 genomic region spanning genes *fusR* to *tar* is highly similar between strain Bp 1106a

153 and our target strain Bp 1026b (identity = 99.4%). The RNA-Seq reads were pooled and  
154 then mapped to the genome of strain 1106a using Bowtie2, which allows two base-pair  
155 mismatch [23]. The RNA-Seq read density at each genomic position was visualized by  
156 the UCSC genome browser [22] to determine putative transcription boundaries of *fusR*  
157 and *bucI8*. Sigma 70 promoters (-10 and -35) were predicted by BPRM [24].  
158 Translation initiation sites (TISs) were predicted by TriTISA with default parameters [25].  
159 The Shine-Dalgarno (SD) translation initiation signals were manually annotated within  
160 20 bps upstream to TISs by considering “GGAG”, a SD consensus sequence annotated  
161 for *Burkholderia* [26]. The gene and protein designation were adopted according to  
162 Crutcher *et al.* 2017.

### 163 **Prediction of *FusR* putative binding sites**

164 The positions of the predicted *FusR* binding sites, a LysR-type transcriptional  
165 regulator, were determined using the University of Braunschweig Virtual Footprint  
166 Promoter analysis tool v3.0 [27]. Known LysR regulators were used as models to  
167 predict binding, including CysB, MetR, and OxyR from *E. coli*, GltC from *Bacillus*  
168 *subtilis*, and OxyR from *P. aeruginosa*. Standard settings were used to run the  
169 prediction (sensitivity = 0.8, core sensitivity = 0.9, and size = 5) on the 500-bp region  
170 upstream from the translational start site of *bucI8*.

## 171 **Genetic and molecular biology methods**

### 172 **Construction of an unmarked isogenic deletion mutant of *bucI8* locus in Bp82**

173 The chromosomal region in Bp82, encompassing genes *bucI8-fusCD-fusE*, was  
174 deleted using suicide plasmid pSL524 constructed in vector pMo130 (Addgene), as

175 described previously [20]. Two Bp82-DNA fragments of about 1 kb each were  
176 sequentially cloned within the multiple cloning site of pMo130: (i) pSL522 construct,  
177 containing *fusR* gene located upstream of *bucl8* was PCR-amplified with primers  
178 pSL522-ApaI-F and pSL522-HindIII-R, was cloned between *ApaI*-*HindIII* sites of the  
179 vector; and (ii) pSL524, containing *tar* gene located downstream of *fusE* was cloned at  
180 *ApaI* site, following amplification with primers pSL523-ApaI-2F and pSL523-ApaI-2R.

181 Plasmid pSL524 was introduced by conjugation into Bp82 via biparental mating with  
182 a donor strain *E. coli* S17-1 $\lambda$ pir/pLFX::pSL524 on LA medium overnight. The mating  
183 bacteria were then scraped off and plated onto selective LA medium supplemented with  
184 200  $\mu$ g/mL kanamycin, to counter-select WT Bp82, and 50  $\mu$ g/mL zeocin, to counter-  
185 select *E. coli*. Merodiploid colonies resulting from the single cross-over event, were  
186 sprayed with 0.45 M pyrocatechol (Sigma-Aldrich) to detect yellow transconjugants [20].  
187 Several yellow colonies were streaked onto YT medium (10 mg/mL yeast extract, 10  
188 mg/mL tryptone) containing 15% sucrose to force the excision of the *bucl8-fusE* locus  
189 and pMo130 sequence from Bp82 merodiploids. Colonies were grown for 48 hours.  
190 Successful excision produces deletion mutants as white colonies identified by spraying  
191 with pyrocatechol. White colonies were isolated and characterized by PCR and  
192 sequencing to confirm the deletion of the *bucl8-fusCD-fusE* genes.

### 193 **Cloning of *bucl8* locus in *E. coli* JM109**

194 The cloning strategy was based on the genomic sequence of the Bp82 parent strain  
195 *B. pseudomallei* 1026b, which identified a ~8.2-kb *StuI*-*StuI* fragment, encompassing  
196 the entire *fusR-bucl8-fusCD-fusE* locus. Bp82 gDNA was digested with *StuI* and DNA

197 species of about 8-10 kb were isolated from the gel and ligated to *Stu*I-cleaved vector  
198 pUC18T-mini-Tn7T-Tp (pUC18T-mini-Tn7T-Tp was a gift from Heath Damron, Addgene  
199 plasmid # 65024) [19]. The *E. coli* JM109 transformants were isolated on a LA medium  
200 containing 100 µg/mL FA. Plasmid pSL525 was isolated from several colonies and  
201 analyzed by restriction digestion. Junctions between vector and insert sequences were  
202 sequenced to establish insert orientation. The presence of *fusR-bucl8-fusC-fusE* genes  
203 was verified by PCR and sequencing.

204 The plasmid construct pSL529, containing the *bucl8* sequence with extended CL  
205 region from Bp K96243, was also generated based on pSL525. An internal Bucl8  
206 fragment from Bp K9264 (~1.4-kb) was PCR-amplified (using primers Bucl8-1F and  
207 BurkhFusBCD-1R) and cloned between two unique sites in *bucl8*, *Xcml*, and *Fsel*, of  
208 pSL525. *E. coli* JM109 transformants were isolated on a LA medium containing 100  
209 µg/mL ampicillin. The plasmid sequence was verified as before.

### 210 ***Cloning, expression and purification of Bucl8-derived recombinant proteins***

211 Two recombinant polypeptides, derived from the presumed extracellular portions of  
212 Bucl8 variant in Bp K96243, were generated for this study: (i) pSL521-encoded rBucl8-  
213 CL-Ct polypeptide, containing both the collagen-like region and the non-collagen C-  
214 terminal region and (ii) pSL520-encoded rBucl8-Ct, which only includes the C-terminal  
215 region.

216 For cloning, gBlocks (Integrated DNA Technologies) were designed, encoding two  
217 recombinant constructs (**Table S3**), as described [28]. gBlocks were used as templates  
218 to produce cloned DNA inserts using primers pSL521-F and pSL521-2R for pSL521

219 construct, and pSL520-F and pSL520-R for pSL520. gBlock DNA fragments were  
220 inserted between *HindIII* and *BamHI* sites of the pQE-30 vector, resulting in an N-  
221 terminal 6xHis-tag (Qiagen) for each construct and were then cloned into *E. coli* JM109.  
222 Plasmid constructs pSL520 and pSL521 were confirmed by sequencing (Primers  
223 pQE30-F, pQE30-2R).

224 For protein expression, *E. coli* JM109 with pSL520 or pSL521 constructs were grown  
225 in LBM plus 100 µg/mL ampicillin with shaking at 37°C overnight, and then 10 mL  
226 cultures were used to inoculate 1 L batches of the same media. The protein expression  
227 was induced in cultures at OD<sub>600</sub> ~0.5 with 1 mM isopropyl β-d-1-thiogalactopyranoside  
228 for 3 hours and then bacterial cells were pelleted and frozen at -20°C overnight. Cell  
229 pellets were thawed and suspended in 10 mL of lysis buffer (50mM Tris buffer, 50mM  
230 NaCl, 2mM MgCl<sub>2</sub>, 2% Triton X-100, 10mM β-mercaptoethanol, 0.2 mg/mL lysozyme, 1  
231 mL of EDTA free Protease inhibitor Mini tablets (Pierce), 1 mM PMSF, 10 µg/mL). The  
232 samples were vortexed, placed on ice for 20 minutes, and then centrifuged. The  
233 supernatants were applied onto affinity columns with HisPur™ Cobalt Resins (Thermo  
234 Scientific) and purification was carried out according to manufacturer's protocol. The  
235 eluted proteins were analyzed by 4-20% SDS-PAGE to assess the overall integrity and  
236 purity. The proteins were dialyzed in 25 mM HEPES and stored at -20°C.

### 237 **Ligand binding assay to rBucl8-CL-Ct and rBucl8-Ct**

238 In the initial screening assay, binding of the rBucl8-CL-Ct to different extracellular  
239 matrix (ECM) ligands was assessed by ELISA [29]. Wells were coated overnight with 1  
240 µg of each ligand dissolved in bicarbonate buffer: collagen type I and IV (Sigma), elastin

241 (Sigma), fibrinogen (Enzyme Research), plasma fibronectin (Sigma), cellular fibronectin  
242 (Sigma), laminin (Gibco), and vitronectin (Sigma). Next, 1  $\mu$ g per well of rBucl8-CL-Ct in  
243 TBS, 1% BSA was added and incubated for two hours at 37°C. Wells were washed with  
244 TBS and bound rBucl8-CL-Ct was detected with anti-6His-tag mouse mAb (Proteintech)  
245 in TBS-1% BSA and a secondary goat anti-mouse HRP-conjugated Ab (Jackson  
246 Immuno Research Laboratories Inc.); immunoreactivity was detected with ABTS  
247 substrate and measured spectrophotometrically at OD<sub>415</sub>. Data represent the mean  $\pm$ SE  
248 of three independent experiments (n=3), each performed in triplicate wells.  
249 Concentration-dependent binding was assessed in a similar manner, however with  
250 varying concentrations (0-10  $\mu$ M) of rBucl8-CL-Ct.

## 251 **Structural characterization of collagen-like domain**

252 Homology modelling of the collagen-like (CL) region of Bucl8 was performed using  
253 the software MODELLER [30]. As a starting structure, we adopted the high-resolution  
254 structure of a collagen-like peptide (PDB code 1k6f) [31]. The Ct random coil region was  
255 generated using the Molefacture plugin of VMD [32]. Electrostatic potential surface was  
256 computed using the software Chimera [33].

257 Circular dichroism spectroscopy of rBucl8-derived polypeptides was performed as  
258 previously described [28]. Briefly, protein samples were dialyzed against 1x Dulbecco's  
259 phosphate buffered saline, pH 7.4. CD spectra were taken with a Jasco 810  
260 spectropolarimeter, in a thermostatically controlled cuvette, with a path length of 0.5 cm.  
261 Data were acquired at 10 nm per minute. Wavelength scans were performed from 240  
262 nm to 190 nm at either 25°C or 50°C for unfolded triple helix in rBucl8-CL-Ct construct.

## 263 **Gene transcription by RT-qPCR**

264 Duplicated bacterial cultures of Bp82 and CLH001 were grown in broth media at  
265 37°C with shaking till early logarithmic phase ( $OD_{600} \sim 0.4$ ), then, FA was added to one  
266 of each culture at sub-inhibitory concentrations and incubated for one hour. Cultures  
267 were mixed with a 1:2 ratio of RNA Protect reagent, incubated for five minutes, then  
268 centrifuged and decanted. Pellets were suspended in lysing buffer (1.3 µg/µL proteinase  
269 K, 0.65 mg/mL lysozyme, TE; 10 mM Tris, 1mM EDTA, pH 7) and incubated for ten  
270 minutes. Total RNA was isolated using RNeasy Protect Bacteria Mini kit (Qiagen).  
271 TurboDNase enzyme [34] was used to remove traces of genomic DNA. RNA was either  
272 used immediately for cDNA synthesis or stored at -80°C for no more than one week.  
273 cDNA was generated using iScript cDNA synthesis kit (Bio-Rad #1708896).

274 RT-qPCR was performed using SsoAdvanced Universal SYBR Green Supermix  
275 (Bio-Rad), with primers listed in **Table S1**. Transcript levels were normalized to 16S  
276 rRNA [35]. Transcription fold change was calculated as relative to non-FA conditions,  
277 using the  $2^{-\Delta\Delta CT}$  method. Technical and experimental replicates were done in triplicate.

## 278 **Determination of antimicrobial susceptibility/resistance**

### 279 ***Antimicrobial susceptibility by broth dilution method***

280 Minimum inhibitory concentration (MIC) testing was performed in liquid and on solid  
281 media. Initially, Bp82 and CLH001 were grown overnight at 37°C with shaking to  
282 inoculate fresh media with varying concentrations of FA (32 µM to 8000 µM), as

283 described [36]. The optical density was recorded after overnight incubation and colony  
284 forming units (CFU) were calculated after plating serially diluted samples on LA media.

### 285 ***Antimicrobial sensitivity on agar***

286 Strains were also tested for growth on LA media supplemented with differing  
287 concentrations of antimicrobials. Bacterial cultures were grown to an optical density of  
288 ~0.4 and plated on agar, and incubated at 37°C for 48 hours. The following  
289 concentrations of antimicrobials were used: fusaric acid (FA), 100-800 µg/mL [37]; para-  
290 hydroxybenzoic acid (pHBA), 0.5-2.5 mg/mL [38]; and chloramphenicol (CHL), 2-32  
291 µg/mL serially diluted [39].

### 292 ***Antimicrobial susceptibility in clinical laboratory***

293 Strains were tested with antimicrobials in a clinical laboratory using Thermo  
294 Sensititre GNX3F dehydrated 96-well plates (TREK Diagnostic Systems). Bacterial  
295 cultures were grown on LA medium and cells were emulsified in sterile water to turbidity  
296 of 0.5 McFarland. The suspension was then diluted in cation adjusted Mueller-Hinton  
297 broth with TES buffer before inoculation of 100µL (approximately  $5 \times 10^5$  CFU) into each  
298 antimicrobial test well. Plates were incubated for 24 hours at 34-36°C in a non-CO<sub>2</sub>  
299 incubator. Results were read and interpreted based on manufacturer's protocol and  
300 CLSI MIC interpretive guidelines [40]. Antimicrobials tested included: amikacin,  
301 doxycycline, gentamicin, minocycline, tobramycin, tigecycline, ciprofloxacin,  
302 trimethoprim/sulfamethoxazole, levofloxacin, aztreonam, imipenem, cefepime,  
303 meropenem, colistin, polymyxin, ceftazidime, cefotaxime, ampicillin/sulbactam,  
304 doripenem, piperacillin/tazobactam, ticarcillin/clavulanate.



305 Antimicrobial susceptibility was also assessed by disk diffusion using the following  
306 antimicrobials: ampicillin (Am 10), ciprofloxacin (CIP 5), doxycycline (D 30), gentamycin  
307 (GM), trimethoprim/sulfamethoxazole (SXT), tetracycline (TE 30), tobramycin (NN 10),  
308 levofloxacin (LVX 5).

## 309 **Statistical analysis**

310 Statistics were performed using GraphPad Prism software for two-tailed paired  
311 Student's *t*-test, one-way and two-way ANOVA, pending the experiment. For gene  
312 expression of the *bucI8* operon in Bp82, statistical analysis was applied to log-  
313 transformed fold changes to account for the phenomena of heteroscedasticity.  
314 Significance was denoted at levels of \* $p \leq 0.05$ , \*\* $p \leq 0.01$ , \*\*\* $p \leq 0.001$ . Error bars  
315 represent standard error measurements (SEM) with analyses based on three  
316 independent experimental repeats ( $n = 3$ ), each performed in triplicate technical  
317 replicates, unless otherwise noted.

## 318 **Results**

### 319 **Structural characterization of the extended extracellular domain of** 320 **BucI8 indicates triple helix formation**

321 Previously, we had described the domain organization of the protein BucI8, reported  
322 the coding sequence, and homology-modelled the structure of its periplasmic/outer  
323 membrane component, based on the structure of the outer membrane protein OprM of  
324 *P. aeruginosa* [13]. Each mature BucI8 monomer is comprised of two tandem outer  
325 membrane efflux protein domains (OEP1 and OEP2), and a rare repetitive region

326 consisting of glycine, alanine, and serine (GAS)<sub>n</sub> triplet repeats, here denoted as the CL  
327 domain, which is followed by a non-collagen carboxyl-terminal (Ct) region (**Fig 1A**).  
328 Bucl8 is a homotrimeric molecule, which supports triple-helical structure of the  
329 extracellular CL-(GAS)<sub>n</sub> domain, although, the specific (GAS)<sub>n</sub> sequence has not been  
330 studied for triple helix formation. The number of consecutive (GAS)<sub>n</sub> repeats present  
331 fluctuates between Bucl8 variants from different *B. pseudomallei* isolates. Analysis of  
332 ~100 *buc18* alleles showed (GAS)<sub>n</sub> numbers ranging from 6 to 38 repeats (mode: 20).  
333 Notably, 21 consecutive GAS repeats characterize the Bucl8 of *B. pseudomallei* model  
334 strain K96243, while the Bucl8 variants of the strains utilized in this study have fewer  
335 (GAS)<sub>n</sub> numbers, e.g., Bp 1026b/Bp82 has six and *B. mallei* strain Bm ATCC  
336 23344/CLH001 has eight. Following the CL-(GAS)<sub>n</sub> domain is a Ct region of 72 amino  
337 acids that are conserved among *B. pseudomallei* and *B. mallei* strains. (**File S1**)

338 Here, we homology-modelled a representative (GAS)<sub>19</sub> sequence using the structure  
339 of the collagen peptide (PPG<sub>10</sub>)<sub>3</sub> as a template (PDB code 1k6f, seqid 36%) [31] and  
340 the software MODELLER (**Fig 1B**). This structure formed a triple helix of about 163 Å in  
341 length. On its C-terminal end, the Ct domain of each chain is predicted by JPRED to be  
342 unfolded and was modeled in a random coil conformation (**Fig 1B**). Consistent with the  
343 sequence composition of the (GAS)<sub>n</sub> repetitive domain, its electrostatic potential surface  
344 appears neutral, with only a few positive charges due to the presence of arginine  
345 residues in the unstructured Ct regions of the molecule (**Fig 1B**).

346 To experimentally validate this homology-modelled structure, two recombinant  
347 proteins, derived from the extracellular portion of Bucl8 variant in strain Bp K96243,

348 were designed and expressed in *E. coli*. The construct rBucl8-CL-Ct includes the CL-  
349 (GAS)<sub>19</sub> domain and adjacent unstructured C-terminus (Ct), while construct rBucl8-Ct  
350 encompasses the Ct region only. Both Bucl8-derived polypeptides migrate aberrantly in  
351 SDS-PAGE in relation to molecular weight standards, e.g., rBucl8-CL-Ct of expected  
352 11.7 kDa and rBucl8-Ct of 7.8 kDa (**Fig 1C**). Structural analysis of rBucl8-CL-Ct  
353 rendered at 25°C, using circular dichroism spectroscopy, confirmed a triple helical  
354 structure, demonstrated by a shallow peak at 220 nm (**Fig 1D**). As a control, denatured  
355 rBucl8-CL-Ct (50°C line) displayed a further-depressed peak at 220 nm that no longer  
356 held a triple-helical collagen structure. The 220 nm peak in rBucl8-CL-Ct is less  
357 pronounced when compared to typical triple helices formed by perfect GPP collagen  
358 repeats. This feature suggests the coexistence of both triple helix and random coil  
359 structures and/or the contribution of the non-collagen Ct region to the spectrum; such  
360 effects on CD spectra were previously reported for streptococcal collagen-like rScl  
361 constructs [41]. Additionally, the rBucl8-Ct structure was also analyzed by circular  
362 dichroism spectroscopy. The absence of ellipticity maxima and/or minima of known  
363 structures, e.g.,  $\alpha$ -helices or  $\beta$ -strands [42], indicates an unstructured protein (**Fig 1D**).  
364 Altogether, using *in silico* modeling and experimental CD spectroscopic analyses of the  
365 representative recombinant protein, we demonstrated that repeating (GAS)<sub>n</sub> of the  
366 predicted Bucl8-CL region from *B. pseudomallei* and *B. mallei* can form a stable  
367 collagen triple helix; to our knowledge, this is the first such demonstration obtained for  
368 the unusual repeating (GAS)<sub>n</sub> collagen-like sequence.

369 Bacterial proteins harboring CL domains from diverse genera have been  
370 demonstrated to bind ligands, including extracellular matrix proteins (ECM), and have

371 been shown to participate in pathogenesis [43-45]. Here, we screened several human  
372 compounds by ELISA to ascertain a potential ligand binding function of Bucl8's  
373 extracellular region, rBucl8-CL-Ct; ligands included fibrinogen, collagen-I and IV, elastin,  
374 plasma and cellular fibronectin, and vitronectin. Of the ligands tested, rBucl8-CL-Ct  
375 construct showed significant binding to fibrinogen, but not to collagen I and elastin (**Fig**  
376 **2A**), while binding to other ligands tested was also not significant (not shown). rBucl8-  
377 CL-Ct binding to fibrinogen-coated wells was concentration-dependent in contrast to  
378 control BSA-coated wells. In addition, rBucl8-Ct construct showed limited level of  
379 binding to fibrinogen in this assay (**Fig 2B**).

## 380 **Identification of *bucl8* operon in *Burkholderia pseudomallei* and**

### 381 ***Burkholderia mallei***

382 Previously, we identified two tandem outer-membrane-efflux-protein (OEP;  
383 PF02321) domains in Bucl8 [13], leading to the current hypothesis that Bucl8 is the  
384 outer membrane component of an efflux pump. Genes encoding efflux pumps are often  
385 clustered in operons that are controlled in *cis* by transcriptional regulators, such as  
386 MexR of *P. aeruginosa* and AmrR of *B. pseudomallei* [46-48]. For this reason, we  
387 examined the genes surrounding *bucl8*, which are described in **Table 2** and depicted in  
388 **Fig 3A**. The locus contains additional efflux-pump associated genes, annotated in the  
389 NCBI database to be involved in fusaric acid (FA) resistance, which we designated here  
390 as '*fus*', as previously proposed [37]. In agreement with genomic annotations, we  
391 recognize that Bucl8 is an outer membrane lipoprotein with a lipid moiety attached via  
392 the N-terminal Cys residue of the mature protein (**Fig 3B**; residue No. 24). In the

393 genome of *B. pseudomallei* 1026b, downstream of *bucI8* (OMP; 594 aa) are: *fusC*,  
394 presumably encoding the inner membrane protein of the pump (IMP; 733 aa), *fusD*,  
395 encoding a small protein with domain of unknown function (DUF; 67 aa), and *fusE*  
396 encoding the periplasmic adaptor protein (PAP; 293 aa). The ATG start codon of *fusD*  
397 overlaps with a stop TGA codon of *fusC*. The direction of the next downstream gene,  
398 *tar*, is opposite to *bucI8-fusCDE* and was presumed by definition to be outside of this  
399 operon. Flanking the locus at the 5' end of *bucI8* is a divergently-oriented gene,  
400 encoding a LysR-type transcriptional regulator (LysR; 313 aa) [49], designated here as  
401 *fusR*. The proximity and opposite orientation of *fusR* gene in relation to the *bucI8-fusE*  
402 genes resembled the typical gene organization described in tripartite efflux pumps with  
403 LysR-type regulators; therefore, we hypothesized *bucI8* transcription to be regulated by  
404 the *fusR* product. Using predictive software and analysis of transcriptome data, the  
405 promoters, transcription initiation sites (TIS), and FusR binding sites were identified in  
406 the intergenic region between *fusR* and *bucI8* (**Fig 3B**). FusR was predicted to have  
407 four binding sites, depicted in the green boxes that overlap with the *bucI8* -10 and -35  
408 sites. The consensus sequence for *B. pseudomallei* is "GGAG", according to the  
409 ProTISA database [25], which matches *bucI8*'s predicted Shine-Dalgarno sequence.  
410 Thus, *fusR-bucI8-fusCD-fusE* constitute a regulon, likely involved in FA resistance. The  
411 *bucI8* locus was also conserved in Bp strain K96243 and Bm ATTC 23344; however,  
412 transcriptional units of *bucI8-fusE* were on the positive strand in the genome of K96243  
413 strain, and on the negative strand in Bp 1026b and Bm ATTC 23344 (**Table 2**).

414

415

**Table 2. Genes and associated identification numbers of *bucI8* locus.**

Gene	Product Annotation	Bp 1026b			Bp K96243			Bm ATTC 23344		
		Locus tag	Protein ID	Genomic position	Locus tag	Protein ID	Genomic position	Locus tag	Protein ID	Genomic position
<i>fusR</i>	Transcriptional regulator	BP1026B_I1940	AFI66557.1	2150545-2151486	BPS_R_S10485	WP_0045_34689.1	2345922-2346863	BMA_RS_04430	WP_0041_91155.1	987878-988819
<i>bucI8</i>	RND efflux system, outer membrane lipoprotein, NodT family protein	BP1026B_I1941	AFI66559.1	2151644-2153428	BPS_R_S10490	WP_1624_86666.1	2347036-2348973	BMA_RS_04425	WP_0249_00385.1	985939-987705
<i>fusC</i>	Fusaric acid resistance protein	BP1026B_I1942	AFI66560.1	2153445-2155646	BPS_R_S10495	WP_0099_37757.1	2348990-2351191	BMA_RS_04420	WP_0041_92976.1	983721-985922
<i>fusD</i>	Hypothetical protein	BP1026B_I1943	AFI66561.1	2155643-2155846	BPS_R_S10500	WP_0041_91885.1	2351188-2351391	BMA_RS_04415	WP_0041_91885.1	983521-983724
<i>fusE</i>	Fusaric acid resistance protein <i>fusE</i>	BP1026B_I1944	AFI66562.1	2155860-2156741	BPS_R_S10505	WP_0045_34908.1	2351405-2352286	BMA_RS_04410	WP_0041_91342.1	982626-983507
<i>tar</i>	Methyl-accepting chemotaxis protein	BP1026B_I1945	AFI66563.1	2157092-2158768	BPS_R_S10510	WP_0041_96082.1	2352657-2354333	BMA_RS_04405	WP_0041_96082.1	980610-982286

Data were retrieved from NCBI for *B. pseudomallei* 1026b, *B. pseudomallei* K96243, and *B. mallei* ATTC 23344 reference genomes.

## 453 **Fusaric acid increases relative expression of *bucI8*-operon transcripts**

454 We identified a conserved operon associated with the *bucI8* gene that was present  
455 in all *B. pseudomallei* and *B. mallei* genomes analyzed, including the mutant strains  
456 Bp82 and CLH001 used in this study, and had similarity to genes encoding FA  
457 resistance found in other Gram-negative bacteria [15, 16, 37]. We consequently tested  
458 the predicted FA substrate as a transcriptional inducer for genes associated with the  
459 *BucI8*-efflux pump. We first examined MICs for FA resistance in both *B. pseudomallei*  
460 and *B. mallei* strains using a broth dilution method in the range of 32  $\mu\text{M}$  FA to 8000  
461  $\mu\text{M}$ , which was based on an earlier induction data employing GFP reporter construct in  
462 *P. putida* [36]. Here, we established the FA-MIC for Bp82 as 4000  $\mu\text{M}$  (716  $\mu\text{g}/\text{mL}$ ) and  
463 250  $\mu\text{M}$  (44  $\mu\text{g}/\text{mL}$ ) for CLH001.

464 Sub-inhibitory concentrations of FA, e.g., 1000  $\mu\text{M}$  for Bp82 and 60  $\mu\text{M}$  for CLH001  
465 that did not inhibit the growth rates were used in subsequent induction experiments (**Fig**  
466 **4A**). Total RNA was isolated from the cultures of Bp82 and CLH001 that were either  
467 non-treated or treated with FA (1000  $\mu\text{M}$  or 60  $\mu\text{M}$ , accordingly) at  $\text{OD}_{600} \sim 0.4$  for one  
468 hour. Both *fusR* and *bucI8* genes were expressed in non-treated cultures at basal  
469 levels, but transcription of *bucI8* in Bp82 was significantly induced with FA by an  
470 average 82-fold change in relative expression and a 20-fold change of *fusR*, using  $2^{\Delta\Delta\text{Ct}}$   
471 calculations (**Fig 4B**). CLH001 also demonstrated about a four-fold increase for *fusR*  
472 and *bucI8* when induced with 60  $\mu\text{M}$  FA (**Fig 4C**), although this change is comparatively  
473 lower than that recorded in FA-induced Bp82.



474

475 In a following experiment we confirmed the boundaries of the *fusR-bucI8* operon by  
476 RT-qPCR. Results show that transcription levels of *fusR-bucI8-fusC-fusE* were all  
477 significantly upregulated in samples treated with FA, compared to non-treated controls  
478 (*fusR* = 20-fold  $\pm$  1.37; *bucI8* = 82-fold  $\pm$  8.73; *fusC* = 40-fold  $\pm$  2.84; *fusE* = 86-fold  $\pm$   
479 10.65; **Fig 4B**). In contrast, the expression change of *tar* was significantly lower than  
480 genes from the *fusR-bucI8-fusC-fusE* operon and the associated regulatory gene *fusR*  
481 (1.5-fold  $\pm$  0.03. One-way ANOVA with Tukey's multiple comparison test of the log<sub>10</sub>-  
482 transformed fold change; \*\*\*p < 0.001 for all genes compared to *tar*). This is the first  
483 demonstration of FA-inducible efflux pump in *B. pseudomallei* and *B. mallei*.

#### 484 **A structural analog of fusaric acid pHBA induces pump expression**

485 Previous work reported that FusC-containing FA-exuding pumps were  
486 phylogenetically related to the aromatic carboxylic acid (AaeB) pumps, although it was  
487 unknown whether AaeB systems extrude FA [37]. Notably, studies in *E. coli* show that  
488 regulated concentrations of an FA-derivative, para-hydroxybenzoic acid (pHBA), inside  
489 bacterial cells is important for balanced metabolism of the aromatic carboxylic acids  
490 [38]. Thus, we hypothesized pHBA would also increase the relative expression of the  
491 *bucI8* operon as FA did. Broth cultures of Bp82 $\Delta$ *bucI8-fusE* were induced with the sub-  
492 inhibitory concentration of 6.25 mM (863  $\mu$ g/mL) pHBA and compared to non-treated  
493 cultures. RT-qPCR data showed in Bp82 pHBA induced a 7-fold  $\pm$  0.26 change in *fusR*,  
494 an 18-fold  $\pm$  0.78 change in *bucI8*, a 19-fold  $\pm$  0.98 change in *fusC*, and a 9-fold  $\pm$  0.52  
495 change in *fusE*. Transcription of *tar* was not significantly affected (1.4 fold  $\pm$  0.006



496 change; One-way ANOVA with Tukey's multiple comparison test of the  $\log_{10}$ -  
497 transformed fold change; \*\*\* $p < 0.001$  for all genes compared to *tar*) (**Fig 4D**). Evidence  
498 that aromatic carboxylic acids can induce transcription of this pump may help elucidate  
499 the broader function of Bucl8-associated pump in *B. pseudomallei* and *B. mallei*.

## 500 **Deletion of and complementation with the Bucl8-pump affect** 501 **sensitivity and resistance to FA and pHBA**

502 In order to demonstrate the function of the Bucl8-pump in various physiological  
503 roles, we used a genetic approach by generating two strains for assessing (i) loss-of-  
504 function and (ii) gain-of function. For loss-of-function, we made an isogenic Bp82 mutant  
505 harboring chromosomal deletion of *bucl8-fusCD-fusE* segment, as described [20].  
506 Plasmid pSL524 (**Table 1**) was constructed in the *E. coli* vector pMo130, which is  
507 suicidal in *Burkholderia*, to generate an unmarked deletion mutant (**Fig 5A**). Construct  
508 pSL524, carrying upstream and downstream sequences flanking *bucl8* locus was  
509 transferred to *B. pseudomallei* Bp82 via biparental mating. Deletion was achieved in a  
510 two-step insertion/excision process, as detailed in Materials and Methods section.  
511 Successful deletion of the *bucl8-fusCD-fusE* segment from the chromosome was  
512 confirmed by PCR (**Fig 5B**) and sequencing. We did not delete the *fusR* gene on  
513 purpose to avoid a possible global regulatory effect associated with unknown FusR  
514 function.

515 To exhibit gain-of function, we complemented a heterologous *E. coli* host *in-trans*  
516 with a plasmid construct pSL525 (**Table 1**) harboring the whole *bucl8* locus, generated  
517 in a mini-transposon vector pUC18T-mini-Tn7T-Tp, as depicted in **Fig 5C**. JM109::525

518 transformants were selected on agar containing 100 µg/mL FA and cloning was verified  
519 by PCR (**Fig 5D**) and sequencing. Since Bp82 represents the 1026b strain harboring  
520 Bucl8 variant with (GAS)<sub>6</sub> repeats in the CL region, we made an additional construct,  
521 pSL529, that contains (GAS)<sub>21</sub> repeats, to represent the majority of *B. pseudomallei*  
522 strains, by extending the number of GAS triplets in pSL525.

523 MICs were determined for bacterial growth on LA plates containing FA or pHBA  
524 chemicals, ranging from 0 to 800 µg/mL FA and 500-2,500 µg/mL pHBA (**Fig 6A**). There  
525 was a 4-fold decrease in MIC to FA from 400 µg/mL to 100 µg/mL recorded for  
526 Bp82Δ*bucl8-fusE* mutant compared to the parental Bp82 strain. A similar effect was  
527 observed for pHBA; the MIC for Bp82 was 1500 µg/mL which decreased to 1000 µg/mL  
528 in the mutant. A 12-fold increased MIC on the LA medium with FA was recorded in *E.*  
529 *coli* JM109::525 and JM109::529 (MIC = 300 µg/mL) compared with the JM109 (MIC =  
530 25 µg/mL) recipient. Interestingly, complementation with Bucl8-pump, however, did not  
531 increase the MIC for pHBA above 1000 µg/mL for JM109::525 or JM109:529 strains.

532 Although deletion of the Bucl8 pump resulted in a drastically decreased MIC,  
533 Bp82Δ*bucl8-fusE* mutant still maintained residual level of FA resistance (100  
534 µg/mL). Therefore, we hypothesized that additional proteins annotated as FusC are  
535 contributing to the remaining FA resistance recorded in the Bp82Δ*bucl8-fusE* mutant.  
536 Within Bp 1026b and K96243 genomes, there are six genes present that are annotated  
537 as FusC-type proteins (Pfam #PF04632), including the protein arbitrarily designated as  
538 FusC, which is associated with Bucl8, whereas remaining five were designated FusC 2  
539 thru FusC 6 (**Table S2**). These protein sequences ranged roughly in three different

540 lengths: ~200 amino acids for FusC 3, ~350 for FusC 4 and 6, and ~750 amino acids for  
541 FusC, FusC 2 and FusC 5. Upon examination, the loci around FusC genes 2 thru 6  
542 were not arranged in as discernable tripartite-pump operons, like FusC, although some  
543 were adjacent to either a MFS transporter protein or genes encoding amino acid  
544 permeases. To test whether these genes are regulated by FA addition, we performed  
545 RT-qPCR on RNA isolated from Bp82 cultures induced with 1000  $\mu$ M FA and without  
546 treatment. The transcription of *fusC* 2-6 genes showed little to no fold-change (0- 2-fold;  
547 **Fig 6B**) when compared to non-treated samples, which contrasts with ~40-fold  
548 difference in *fusC* transcription (**Fig. 4B**). Thus, we conclude that these *fusC* genes are  
549 not inducible by FA.

## 550 **Bucl8-pump does not contribute to the multidrug resistance (MDR)** 551 **phenotype**

552 Efflux pumps contribute to MDR in Gram-negative bacteria [11], including  
553 *Burkholderia* species [8], and are often polyspecific [51]. A study in *S. maltophilia*  
554 concluded that an FA efflux pump did not extrude the antimicrobials tested [50]. Here,  
555 we assessed changes in resistance/ susceptibility levels between Bp82 and  
556 Bp82 $\Delta$ *bucl8-fusE*, and JM109 and JM109::525 or JM109:529 against variety of  
557 antimicrobials.

558 In the clinical laboratory setting, the *Burkholderia* failed to grow in commercial  
559 medium, and therefore only the *E. coli* data were generated. Overall, there was not a  
560 significant increase in resistance to any of the antibiotics tested; JM109::525/529  
561 showed only increased resistance to the  $\beta$ -lactam antibiotics, which was associated with

562 the resistance gene present on the inserted plasmid. A disc diffusion test, including  
563 ampicillin, ciprofloxacin, levofloxacin, tobramycin, gentamicin, tetracycline, doxycycline,  
564 and trimethoprim-sulfamethoxazole, resulted in similar zones of inhibition for both Bp82  
565 and Bp82 $\Delta$ *bucI8-fusE* cultures, as well as *E. coli* JM109 and JM109::525/529, again  
566 with the exception of the plasmid-derived  $\beta$ -lactam resistance determinate.

567 Microarray data comparing the effect of 84 growth conditions on *B. pseudomallei*  
568 transcriptome showed that chloramphenicol (CHL), which contains an aromatic ring in  
569 its structure, induced *bucI8* expression, thus, implying CHL might be a substrate for  
570 Bucl8-associated pump [52]. Here, we determined the CHL-MICs of our *B.*  
571 *pseudomallei* and *E. coli* strains using a growth assay on the LA medium; however, the  
572 MIC for all the strains was the same (8  $\mu$ g/mL; **Fig 6A**). In addition, the exogenous CHL  
573 at 8  $\mu$ g/mL or 4  $\mu$ g/mL concentrations did not significantly induced the transcription of  
574 *bucI8*-associated genes (not shown). Thus, our results indicate the Bucl8-associated  
575 pump is not needed for CHL resistance in *B. pseudomallei* [49].

## 576 **Deletion of Bucl8-pump components affects cell growth**

577 Efflux pumps extrude a variety of compounds that are toxic to the cells and play  
578 physiological functions linked to pathogenesis [12]. We observed the growth of the  
579 Bp $\Delta$ *bucI8-fusE* mutant was considerably reduced than that of the parent Bp82 and did  
580 not reach the same OD<sub>600</sub> in the stationary phase (**Fig 6C**). CFU for Bp82 increased by  
581 approximately four logs, while the mutant increased by two logs from hour 0 to 12. (**Fig**  
582 **6D**). These results suggest that the pump components are needed for normal growth  
583 physiology under laboratory conditions in rich medium.

## 584 Discussion

585 The protein Bucl8 was previously predicted to be the outer membrane in *B.*  
586 *pseudomallei* and *B. mallei*. Comparative genomics studies between *B. mallei* and *B.*  
587 *pseudomallei* have suggested that conserved genes between the species are likely  
588 critical for host-survival, while genes useful for saprophytic life-style and adaptability  
589 were selected against [6]. The presence of the *bucI8* genes, in particular the acquisition  
590 and conservation of the extracellular Bucl8-CL-Ct domain, in *B. pseudomallei* and *B.*  
591 *mallei* suggests that these genes are selected for because they are useful for bacterial  
592 survival in both the environment and in the host. Here, we carried out structure-function  
593 studies of the Bucl8 protein and associated locus in *B. pseudomallei* and *B. mallei* in  
594 order to elucidate the role of Bucl8 and its associated pump components in antimicrobial  
595 resistance, ligand binding, and cell physiology.

596 In the absence of hydroxyprolines that stabilize the triple helical structure of  
597 mammalian collagen, bacterial collagens adopt alternative stabilization mechanisms to  
598 form stable triple helices [53]. While some prokaryotic collagens utilize a variety of GXY-  
599 repeat types, such as streptococcal collagen-like proteins Scl1 and Scl2 [54], others  
600 possess a limited number of triplets, including *Bacillus* Bcl proteins [55, 56]. The CL  
601 regions of various Bucl proteins utilize relatively few distinct triplet types [13]. An  
602 extreme case is the Bucl8-CL region, which is exclusively made of a rare repeating  
603 (GAS)<sub>n</sub> sequence. Our results are consistent with studies of triple helix propensity  
604 based on host-guest peptide studies, showing reasonable propensities of (GAS)<sub>n</sub> triplets  
605 to form triple helical structures. The T<sub>m</sub> value of (GAS)<sub>n</sub> tripeptide unit in a triple helix is  
606 33.0°C, compared to 47.3°C of (POG)<sub>n</sub> tripeptide (O is hydroxyproline), although, the

607 physical anchoring of a CL domain increases  $T_m$  by additional 2°C [57]. This relatively  
608 low  $T_m$  may suggest structural flexibility of the Bucl8 extracellular domain under  
609 physiological conditions, thus, allowing efflux pump for dual function.

610 Our laboratory and others have shown that bacterial collagen-like proteins  
611 participate in pathogenesis via a variety of functions, including immune evasion, cell  
612 adhesion, biofilm formation, and autoaggregation [43-45, 58]. Here, we report that the  
613 recombinant rBucl8-CL-Ct polypeptide binds to fibrinogen significantly better than  
614 rBucl8-Ct polypeptide. A similar phenomenon was recently reported for Scl1, where the  
615 effective binding to fibronectin, directly mediated by the globular V domain, required the  
616 presence of adjacent Scl1-CL domain [28]. Fibrinogen is a circulating glycoprotein that  
617 is involved in blood clotting and promoting wound healing [59]; we do not know the  
618 location of Bucl8 binding site on this multidomain protein. In the scope of pathogenesis,  
619 some Gram-negative and Gram-positive bacteria use fibrinogen for biofilm formation  
620 and bacterial adhesion. For example, fibrinogen-binding factors and clumping-factors of  
621 *Staphylococcus aureus* have been shown to increase adherence and virulence [60-62].  
622 *B. pseudomallei* and *B. mallei* both cause cutaneous infections that lead to lesions and  
623 nodules, thus binding to wound factors could increase colonization. In addition, it is  
624 likely that unidentified ligand(s), other than fibrinogen, may exist in the environment to  
625 support a saprophytic lifestyle of *B. pseudomallei*.

626 *buc18*-operon expression is regulated by a LysR-type transcriptional regulator,  
627 designated here as FusR<sub>LysR</sub>. LysR-type family regulators are the most abundant class  
628 of the prokaryotic transcriptional regulators that monitor the expression of genes

629 involved in pathogenesis, metabolism, quorum sensing and motility, toxin production,  
630 and more physiological and virulence traits [49]. LysR proteins are tetrameric and  
631 consist of two dimers that bind and bend the DNA within promoter regions, thus,  
632 affecting the gene transcription. After the co-inducer binds to the LysR dimers, the DNA  
633 is relaxed, allowing one dimer to come into contact with the RNA polymerase to form an  
634 active transcription complex. In this study, the FusR binding sites were identified within  
635 the intergenic promoter region between *bucI8* and *fusR* in *B. pseudomallei* and *B.*  
636 *mallei*. Thus, we hypothesized that FA can act as a co-inducer for the *bucI8*-operon.

637 We show that exogenous fusaric acid (FA) induces the transcription of the *fusR*-  
638 *bucI8-fusCD-fusE* operon, therefore, confirming *BucI8* is a component of a previously  
639 unreported FA-inducible efflux pump in *B. pseudomallei* and *B. mallei*. Similarly, an  
640 inducible FA tripartite efflux pump, encoded by *fuaABC* operon, was identified in  
641 another soil saprophyte *S. maltophilia* [50]. However, the gene/protein arrangement,  
642 e.g. sequence orientation and length, places the *bucI8* operon within clade III of a  
643 phylogenetic tree of predicted FusC-associated operons, while *fuaABC* operon is in  
644 clade IV [37]. In addition to FA, the FA-derivative pHBA also induced the expression of  
645 the *bucI8* operon. Interestingly, although the genes and intergenic regions are highly  
646 similar, transcription of *fusR* and *bucI8* in FA-induced *B. mallei* culture is considerably  
647 reduced compared to *B. pseudomallei*. Likewise, the MIC levels for FA and pHBA were  
648 lower in *B. mallei*, although the *bucI8* loci are conserved between *B. pseudomallei*  
649 1026b and *B. mallei* ATCC23344. There may be other factors affecting transcription,  
650 such as additional regulatory circuits for processing FA and similar compounds in both  
651 organisms. For similarity, another efflux pump in *B. pseudomallei*, *BpeEF-OprC*, is



652 regulated by two highly similar LysR-type transcriptional regulators, BpeT and BpeS  
653 [63]. Further studies are needed to identify if there are other regulators or environmental  
654 stress/factors that could be affecting upstream/downstream targets.

655 Efflux systems are categorized into families by their structure – including their  
656 composition, conserved domains, and number of transmembrane spanning regions – as  
657 well as by their energy source and substrates. In *Fusarium*, the synthesized intracellular  
658 FA is extruded by a predicted MFS-type transporter FUBT [64], however based on the  
659 number of amino acids present and transmembrane helices, FusC is not likely a MFS  
660 transporter. Only ABC or RND systems regularly form tripartite complexes. It is not  
661 known whether the Bucl8 pump relies on ATP hydrolysis to transport FA, but the  
662 associated FusC<sub>IMP</sub> transporter does not contain an ATP-binding domain, therefore, it is  
663 an unlikely an ABC-transporter. Phylogenetic analysis of bacterial efflux systems  
664 implied that FuaABC tripartite FA efflux pump in *S. maltophilia* forms a separate branch  
665 from other bacterial efflux pump families, branching off between the ABC and RND  
666 families [50]. Thus, we construe that the Bucl8 associated efflux pump is RND-like.

667 Here, we adopted the gene designation proposed by Crutcher *et al.*, which also  
668 includes a fourth pump component, a small polypeptide DUF, for the Bucl8-associated  
669 tetrapartite efflux system. This situation might be more common among known tripartite  
670 efflux pumps than currently acknowledged; for example, a small polypeptide YajC is an  
671 inner membrane component of a well-recognized “tripartite” RND system AcrAB-TolC  
672 [65]. Another known tetrapartite RND efflux system is the CusCFBA complex, which  
673 transports heavy metals copper and silver [66]. In this system, the small CusF



674 component serves as a periplasmic metal-binding chaperone, which hands over the  
675 metal-ion substrate to the IMP transporter [67, 68]. The precise cellular location and  
676 function of FusD<sub>DUF</sub> protein is not known at present.

677 Early studies reported FA-detoxification genes found in *Burkholderia* (formerly  
678 *Pseudomonas*) *cepacia* and *Klebsiella oxytoca* [15, 16], which were attributed to FA  
679 resistance. More recent work identified a tripartite FA efflux pump, FuaABC, in  
680 *Stenotrophomonas maltophilia* [50], while other work distinguished a large number of  
681 the phylogenetically related FusC-type proteins, conferring FA resistance, in numerous  
682 Gram-negative bacterial species [37]. Not all FusC proteins were predicted components  
683 of FA efflux pumps; however they were assumed to be contributing to high levels of FA  
684 resistance in some species, including *Burkholderia*. Crutcher *et al.* reported positive  
685 correlation between the number of putative FusC proteins in bacterial genomes and the  
686 level of resistance to FA; for example, *Burkholderia cepacia*, harboring six predicted  
687 FusC proteins, had a FA-MIC of  $\geq 500$   $\mu\text{g/mL}$ , whereas *Burkholderia glumae* had two  
688 FusC proteins and a FA-MIC of 200  $\mu\text{g/mL}$  [37]. Strains with 0-1 *fusC* genes were  
689 sensitive to FA with MIC  $< 50$   $\mu\text{g/mL}$ . We also observed that our Bp82 $\Delta$ *bucI8-fusE*  
690 mutant retained 100  $\mu\text{g/mL}$  residual resistance to FA. Through transcriptional analysis,  
691 we found that the five *fusC*/FusC genes/proteins outside of the *BucI8*-operon showed  
692 little to no induction, indicating that the *BucI8* pump is the main contributor to FA  
693 resistance in *B. pseudomallei*.

694 The multidrug resistance in *B. pseudomallei* is substantially attributed to previously  
695 studied RND efflux pumps BpeAB-OprB, AmrAB-OprA, and BpeEF-OprC. At the same

696 time, little is known about the role of FA pumps in resistance against clinically used  
697 drugs. In our studies, we assessed the Bucl8-pump's role in multidrug resistance in two  
698 ways: (i) we compared the spectrum of resistance between parental strain Bp82 and  
699 Bucl8-pump deletion mutant, and (ii) we expressed the *bucI8*-operon in a sensitive *E.*  
700 *coli* strain. Although MICs for FA changed as predicted, deletion of the Bucl8-pump did  
701 not affect MIC values for the clinically-used drugs. This result is comparative to an FA  
702 pump in *S. maltophilia*, which did not determine the resistance to a large panel of  
703 therapeutics tested [50]. At the same time, a different study in the same organism  
704 showed that deletion of the *pcm-tolCsm* operon, encoding a different efflux pump,  
705 resulted in decreased MICs for several antimicrobials of diverse classes ( $\beta$ -lactams,  
706 chloramphenicol, quinolone, tetracycline, aminoglycosides, macrolides), and also  
707 decreased FA resistance [69]. Microarray data suggested *bucI8* expression was  
708 upregulated in the presence of chloramphenicol [52] and deletion of the *tolCsm* in *S.*  
709 *maltophilia* resulted in decreased resistance to both CHL and FA [69]. Both CHL and FA  
710 harbor aromatic rings in their structures, however, our investigations did not detect  
711 *bucI8*-operon induction by CHL nor changes in CHL resistance levels in Bp82 $\Delta$ *bucI8*-  
712 *fusE* mutant or complemented *E. coli*.

713 The decrease in bacterial growth of the Bp82 $\Delta$ *bucI8-fusE* mutant suggests that the  
714 Bucl8-pump may be involved in modulating essential cellular stresses, both in the  
715 environment and in infected human host [12]. Limited studies show that FA repressed  
716 quorum sensing genes, expression of stress factors, secretion of siderophores,  
717 production of anti-fungal metabolites, and iron uptake [70-73]. Additionally, Bucl8 pump  
718 may be involved in a transport of aromatic carboxylic acid compounds and act as a

719 pHBA-metabolic efflux valve [38]. Further investigation will be needed to determine what  
720 cellular processes are associated with the Bucl8-pump.

721 In summary, we conclude that Bucl8 is a component of a previously unreported  
722 tetrapartite efflux system that is involved in FA resistance and cell physiology. We have  
723 demonstrated that the extracellular Bucl8-CL domain forms the prototypic collagen  
724 triple-helix, while the extracellular Bucl8-CL-Ct portion is capable of binding to  
725 fibrinogen. Further studies will investigate what role fibrinogen binding plays in  
726 pathogenesis. While the Bucl8-pump is likely not be involved in the MDR phenotype of  
727 *Burkholderia*, we have identified FA and pHBA as inducible substrates of the pump and  
728 will continue to investigate metabolite analogs that may affect cell function. Importantly,  
729 the growth of the Bucl8-pump deletion mutant was significantly affected even in the  
730 absence of FA and pHBA. By characterizing the Bucl8-associated efflux system, we can  
731 advance therapies and strategies for combating these pathogens, including developing  
732 pump inhibitors, targeting transport mechanisms, or identifying potential surface-  
733 exposed vaccine targets derived from Bucl8.

734

## 735 **Acknowledgements:**

736 We would like to thank Heath Damron for providing us pUC18T-mini-Tn7T-Tp  
737 vector, Alfredo Torres for providing *B. mallei* CLH001, Shelby Bradford for her  
738 assistance with initial experiments, and Paul Feustel for advice with statistical analyses.

739 Opinions, interpretations, conclusions, and recommendations are those of the  
740 authors and are not necessarily endorsed by the US Army.

## 741 **References**

- 742 1. Currie BJ. *Burkholderia pseudomallei* and *Burkholderia mallei*: melioidosis and glanders.  
743 Mandell, Douglas and Bennett's Principles and Practice of Infectious Diseases 7th edn  
744 Philadelphia: Churchill Livingstone Elsevier. 2010:2869-85.
- 745 2. Limmathurotsakul D, Golding N, Dance DAB, Messina JP, Pigott DM, Moyes CL, et al.  
746 Predicted global distribution of *Burkholderia pseudomallei* and burden of melioidosis. Nat  
747 Microbiol. 2016;1(1):1-5. Epub 2016/01/11. doi: 10.1038/NMICROBIOL.2015.8. PubMed  
748 Central PMCID: PMC4746747.
- 749 3. Birnie E, Virk HS, Savelkoel J, Spijker R, Bertherat E, Dance DAB, et al. Global burden of  
750 melioidosis in 2015: a systematic review and data synthesis. Lancet Infect Dis.  
751 2019;19(8):892-902. Epub 2019/07/10. doi: 10.1016/S1473-3099(19)30157-4. PubMed  
752 PMID: 31285144; PubMed Central PMCID: PMC6867904.
- 753 4. Nathan S, Chieng S, Kingsley PV, Mohan A, Podin Y, Ooi MH, et al. Melioidosis in Malaysia:  
754 Incidence, clinical challenges, and advances in understanding pathogenesis. Trop Med  
755 Infect Dis. 2018;3(1). doi: 10.3390/tropicalmed3010025. PubMed PMID: 30274422; PubMed  
756 Central PMCID: PMC6136604.
- 757 5. Inglis TJ. The Treatment of Melioidosis. Pharmaceuticals (Basel). 2010;3(5):1296-303. doi:  
758 10.3390/ph3051296. PubMed PMID: 27713302; PubMed Central PMCID: PMC4033981.
- 759 6. Losada L, Ronning CM, DeShazer D, Woods D, Fedorova N, Kim HS, et al. Continuing  
760 evolution of *Burkholderia mallei* through genome reduction and large-scale rearrangements.  
761 Genome Biol Evol. 2010;2:102-16. Epub 2010/03/25. doi: 10.1093/gbe/evq003. PubMed  
762 PMID: 20333227; PubMed Central PMCID: PMC4033981.
- 763 7. Li X-Z, Plésiat P, Nikaido H. The challenge of efflux-mediated antibiotic resistance in Gram-  
764 negative bacteria. Clin Microbiol Rev. 2015;28(2):337-418. doi: 10.1128/cmr.00117-14.  
765 PubMed PMID: 25788514; PubMed Central PMCID: PMC4402952.
- 766 8. Rhodes KA, Schweizer HP. Antibiotic resistance in *Burkholderia* species. Drug Resist  
767 Updat. 2016;28:82-90. Epub 2016/09/14. doi: 10.1016/j.drug.2016.07.003. PubMed PMID:  
768 27620956; PubMed Central PMCID: PMC4402952.

- 769 9. Gugliera P, Pasca MR, De Rossi E, Buroni S, Arrigo P, Manina G, et al. Efflux pump  
770 genes of the resistance-nodulation-division family in *Burkholderia cenocepacia* genome.  
771 BMC Micro. 2006;6:66-. doi: 10.1186/1471-2180-6-66. PubMed PMID: 16857052; PubMed  
772 Central PMCID: PMCPMC1557404.
- 773 10. Podnecky NL, Rhodes KA, Schweizer HP. Efflux pump-mediated drug resistance in  
774 *Burkholderia*. Front in Microbiol. 2015;6:305. Epub 2015/04/14. doi:  
775 10.3389/fmicb.2015.00305. PubMed PMID: 25926825; PubMed Central PMCID:  
776 PMCPMC4396416.
- 777 11. Vargiu AV, Pos KM, Poole K, Nikaido H. Editorial: Bad Bugs in the XXIst century:  
778 Resistance mediated by multi-drug efflux pumps in Gram-negative bacteria. Front Microbiol.  
779 2016;7:833. Epub 2016/06/16. doi: 10.3389/fmicb.2016.00833. PubMed PMID: 27303401;  
780 PubMed Central PMCID: PMCPMC4885826.
- 781 12. Piddock LJ. Multidrug-resistance efflux pumps - not just for resistance. Nat Rev Microbiol.  
782 2006;4(8):629-36. doi: 10.1038/nrmicro1464. PubMed PMID: 16845433.
- 783 13. Bachert BA, Choi SJ, Snyder AK, Rio RVM, Durney BC, Holland LA, et al. A unique set of  
784 the *Burkholderia* collagen-like proteins provides insight into pathogenesis, genome evolution  
785 and niche adaptation, and infection detection. PLoS ONE. 2015;10(9):e0137578. Epub  
786 2015/09/15. doi: 10.1371/journal.pone.0137578. PubMed PMID: 26356298; PubMed Central  
787 PMCID: PMCPMC4565658.
- 788 14. Ramachandran GN. Stereochemistry of collagen. Int J Pept Protein Res. 1988;31(1):1-16.  
789 Epub 1988/01/01. PubMed PMID: 3284833.
- 790 15. Utsumi R, Yagi T, Katayama S, Katsuragi K, Tachibana K, Toyoda H, et al. Molecular  
791 cloning and characterization of the fusaric acid-resistance gene from *Pseudomonas*  
792 *cepacia*. Agr and Biol Chem. 1991;55(7):1913-8. Epub 2014/09/08. doi:  
793 10.1271/bbb1961.55.1913. PubMed PMID: 1370369.
- 794 16. Toyoda H, Katsuragi K, Tamai T, Ouchi S. DNA sequence of genes for detoxification of  
795 fusaric acid, a wilt-inducing agent produced by *Fusarium* species. J Phytopathology.  
796 1991;133(4):265-77. doi: 10.1111/j.1439-0434.1991.tb00162.x. PubMed PMID: 002064443.
- 797 17. Propst KL, Mima T, Choi K-H, Dow SW, Schweizer HP. A *Burkholderia pseudomallei*  $\Delta$ *purM*  
798 mutant is avirulent in immunocompetent and immunodeficient animals: candidate strain for  
799 exclusion from select-agent lists. Infect and Immun. 2010;78(7):3136-43. doi:  
800 10.1128/iai.01313-09. PubMed PMID: 20404077; PubMed Central PMCID:  
801 PMCPMC2897367.
- 802 18. Hatcher CL, Mott TM, Muruato LA, Sbrana E, Torres AG. *Burkholderia mallei* CLH001  
803 attenuated vaccine strain is immunogenic and protects against acute respiratory glanders.  
804 Infect and Immun. 2016;84(8):2345-54. doi: 10.1128/iai.00328-16. PubMed PMID:  
805 27271739; PubMed Central PMCID: PMCPMC4962637.
- 806 19. Choi KH, Schweizer HP. mini-Tn7 insertion in bacteria with single attTn7 sites: example  
807 *Pseudomonas aeruginosa*. Nat Protoc. 2006;1(1):153-61. Epub 2007/04/05. doi:  
808 10.1038/nprot.2006.24. PubMed PMID: 17406227.
- 809 20. Hamad MA, Zajdowicz SL, Holmes RK, Voskuil MI. An allelic exchange system for compliant  
810 genetic manipulation of the select agents *Burkholderia pseudomallei* and *Burkholderia*  
811 *mallei*. Gene. 2009;430(1):123-31. doi: 10.1016/j.gene.2008.10.011. PubMed PMID:  
812 19010402; PubMed Central PMCID: PMCPMC2646673.

- 813 21. Price EP, Viberg LT, Kidd TJ, Bell SC, Currie BJ, Sarovich DS. Transcriptomic analysis of  
814 longitudinal *Burkholderia pseudomallei* infecting the cystic fibrosis lung. *Microb Genom.*  
815 2018;4(8):e000194. Epub 2018/07/10. doi: 10.1099/mgen.0.000194. PubMed PMID:  
816 29989529.
- 817 22. Chan PP, Holmes AD, Smith AM, Tran D, Lowe TM. The UCSC Archaeal Genome Browser:  
818 2012 update. *Nucleic Acids Res.* 2012;40(Database issue):D646-52. Epub 2011/11/15. doi:  
819 10.1093/nar/gkr990. PubMed PMID: 22080555; PubMed Central PMCID:  
820 PMCPMC3245099.
- 821 23. Langdon WB. Performance of genetic programming optimised Bowtie2 on genome  
822 comparison and analytic testing (GCAT) benchmarks. *BioData Min.* 2015;8(1):1. Epub  
823 2015/01/27. doi: 10.1186/s13040-014-0034-0. PubMed PMID: 25621011; PubMed Central  
824 PMCID: PMCPMC4304608.
- 825 24. Solovyev V, Salamov A. Automatic annotation of microbial genomes and metagenomic  
826 sequences, in Li, R. W., ed., *Metagenomics and its applications in agriculture, biomedicine*  
827 *and environmental studies.* Nova Biomedical. 2011:61-78.
- 828 25. Hu GQ, Zheng X, Zhu HQ, She ZS. Prediction of translation initiation site for microbial  
829 genomes with TriTISA. *Bioinformatics.* 2009;25(1):123-5. Epub 2008/11/19. doi:  
830 10.1093/bioinformatics/btn576. PubMed PMID: 19015130.
- 831 26. Hu GQ, Zheng X, Yang YF, Ortet P, She ZS, Zhu H. ProTISA: a comprehensive resource for  
832 translation initiation site annotation in prokaryotic genomes. *Nucleic Acids Res.*  
833 2008;36(Database issue):D114-9. Epub 2007/10/19. doi: 10.1093/nar/gkm799. PubMed  
834 PMID: 17942412; PubMed Central PMCID: PMCPMC2238952.
- 835 27. Munch R, Hiller K, Grote A, Scheer M, Klein J, Schobert M, et al. Virtual Footprint and  
836 PRODORIC: an integrative framework for regulon prediction in prokaryotes. *Bioinformatics.*  
837 2005;21(22):4187-9. Epub 2005/08/20. doi: 10.1093/bioinformatics/bti635. PubMed PMID:  
838 16109747.
- 839 28. McNitt DH, Choi SJ, Keene DR, Van De Water L, Squeglia F, Berisio R, et al. Surface-  
840 exposed loops and an acidic patch in the Scl1 protein of group A *Streptococcus* enable Scl1  
841 binding to wound-associated fibronectin. *J Biol.* 2018;293(20):7796-810. doi:  
842 10.1074/jbc.RA118.002250.
- 843 29. Caswell CC, Oliver-Kozup H, Han R, Lukomska E, Lukomski S. Scl1, the multifunctional  
844 adhesin of group A *Streptococcus*, selectively binds cellular fibronectin and laminin, and  
845 mediates pathogen internalization by human cells. *FEMS Microbiol Lett.* 2010;303(1):61-8.  
846 Epub 2009/12/17. doi: 10.1111/j.1574-6968.2009.01864.x. PubMed PMID: 20002194;  
847 PubMed Central PMCID: PMCPMC2910189.
- 848 30. Benjamin W, Andrej S. Comparative Protein Structure Modeling Using MODELLER. *Curr*  
849 *Protoc in Bioinformatics.* 2014;47(1):5.6.1-5.6.32. doi: doi:10.1002/0471250953.bi0506s47.  
850 PubMed PMID: 25199792.
- 851 31. Berisio R, Vitagliano L, Mazzarella L, Zagari A. Crystal structure of the collagen triple helix  
852 model [(Pro-Pro-Gly)<sub>10</sub>]<sub>3</sub>. *Protein Sci.* 2002;11(2):262-70. Epub 2002/01/16. doi:  
853 10.1110/ps.32602. PubMed PMID: 11790836; PubMed Central PMCID: PMCPMC2373432.
- 854 32. Yahyavi M, Falsafi-Zadeh S, Karimi Z, Kalatari G, Galehdari H. VMD-SS: A graphical user  
855 interface plug-in to calculate the protein secondary structure in VMD program.



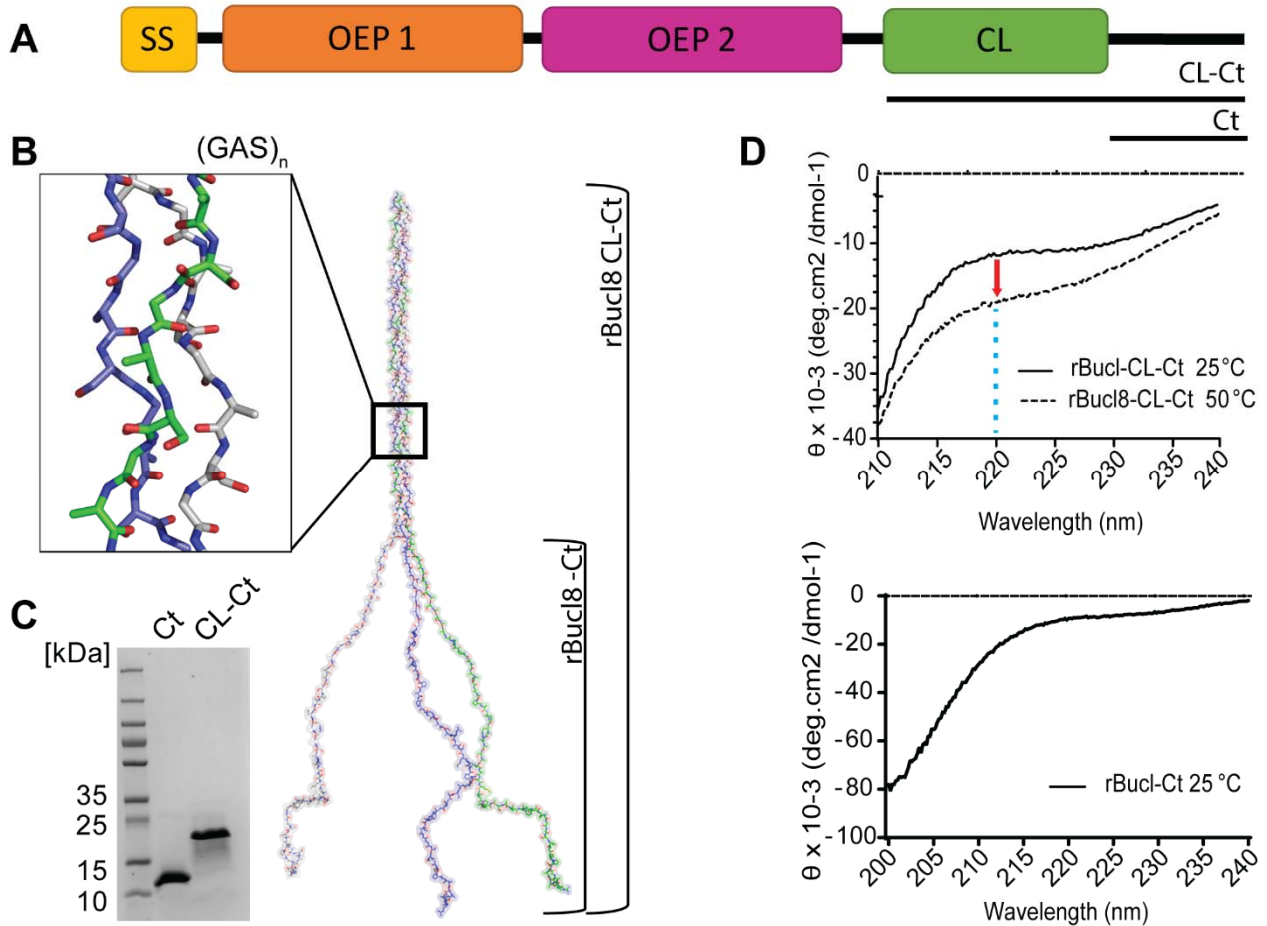
- 856 Bioinformation. 2014;10(8):548-50. Epub 2014/09/27. doi: 10.6026/97320630010548.  
857 PubMed PMID: 25258493; PubMed Central PMCID: PMC4166777.
- 858 33. Pettersen EF, Goddard TD, Huang CC, Couch GS, Greenblatt DM, Meng EC, et al. UCSF  
859 Chimera--a visualization system for exploratory research and analysis. J Comput Chem.  
860 2004;25(13):1605-12. Epub 2004/07/21. doi: 10.1002/jcc.20084. PubMed PMID: 15264254.
- 861 34. Quoilin S, Lambion N, Mak R, Denis O, Lammens C, Struelens M, et al. Soft tissue  
862 infections in Belgian rugby players due to *Streptococcus pyogenes* emm type 81. Euro  
863 Surveill. 2006;11(12):E061221.2.
- 864 35. Sirijant N, Sermswan RW, Wongratanacheewin S. *Burkholderia pseudomallei* resistance to  
865 antibiotics in biofilm-induced conditions is related to efflux pumps. J Med Microbiol.  
866 2016;65(11):1296-306. doi: doi:10.1099/jmm.0.000358. PubMed PMID: 27702426.
- 867 36. Rosmalen Rv. Fungal Sensing 2014. iGEM Wageningen UR 2014]. Available from:  
868 [http://2014.igem.org/Team:Wageningen\\_UR/project/fungal\\_sensing](http://2014.igem.org/Team:Wageningen_UR/project/fungal_sensing).
- 869 37. Crutcher FK, Puckhaber LS, Stipanovic RD, Bell AA, Nichols RL, Lawrence KS, et al.  
870 Microbial resistance mechanisms to the antibiotic and phytotoxin fusaric acid. J Chem Ecol.  
871 2017;43(10):996-1006. doi: 10.1007/s10886-017-0889-x. PubMed PMID: 28986689.
- 872 38. Van Dyk TK, Templeton LJ, Cantera KA, Sharpe PL, Sariaslani FS. Characterization of the  
873 *Escherichia coli* AaeAB efflux pump: a metabolic relief valve? J Bacteriol.  
874 2004;186(21):7196-204. Epub 2004/10/19. doi: 10.1128/jb.186.21.7196-7204.2004.  
875 PubMed PMID: 15489430; PubMed Central PMCID: PMC4166777.
- 876 39. Thibault FM, Hernandez E, Vidal DR, Girardet M, Cavallo J-D. Antibiotic susceptibility of 65  
877 isolates of *Burkholderia pseudomallei* and *Burkholderia mallei* to 35 antimicrobial agents. J  
878 Antimicrob Chemother. 2004;54(6):1134-8. doi: 10.1093/jac/dkh471. PubMed PMID:  
879 15509614.
- 880 40. CLSI. Performance Standards for Antimicrobial Susceptibility Testing. CLSI supplements  
881 M100. 29 ed. Wayne, PA: Clinical and Laboratory Standards Institute; 2019.
- 882 41. Xu Y, Keene DR, Bujnicki JM, Höök M, Lukomski S. Streptococcal Scl1 and Scl2 proteins  
883 form collagen-like triple helices. J Biol Chem. 2002;277(30):27312-8. Epub 2002/04/27. doi:  
884 10.1074/jbc.M201163200. PubMed PMID: 11976327.
- 885 42. Brodsky-Doyle B, Leonard KR, Reid KB. Circular-dichroism and electron-microscopy studies  
886 of human subcomponent C1q before and after limited proteolysis by pepsin. Biochem J.  
887 1976;159(2):279-86. doi: 10.1042/bj1590279. PubMed PMID: 11976327
- 888 43. Duncan C, Prashar A, So J, Tang P, Low DE, Terebiznik M, et al. Lcl of *Legionella*  
889 *pneumophila* is an immunogenic GAG binding adhesin that promotes interactions with lung  
890 epithelial cells and plays a crucial role in biofilm formation. Infect Immun. 2011;79(6):2168-  
891 81. Epub 2011/03/23. doi: 10.1128/iai.01304-10. PubMed PMID: 21422183; PubMed  
892 Central PMCID: PMC3125840.
- 893 44. Paterson GK, Nieminen L, Jefferies JMC, Mitchell TJ. PclA, a pneumococcal collagen-like  
894 protein with selected strain distribution, contributes to adherence and invasion of host cells.  
895 FEMS Microbiol Lett. 2008;285(2):170-6. doi: 10.1111/j.1574-6968.2008.01217.x. PMID:  
896 18557785
- 897 45. Pizarro-Guajardo M, Olguin-Araneda V, Barra-Carrasco J, Brito-Silva C, Sarker MR,  
898 Paredes-Sabja D. Characterization of the collagen-like exosporium protein, BclA1, of

- 899 *Clostridium difficile* spores. *Anaerobe*. 2014;25:18-30. Epub 2013/11/26. doi:  
900 10.1016/j.anaerobe.2013.11.003. PubMed PMID: 24269655.
- 901 46. Poole K, Gotoh N, Tsujimoto H, Zhao Q, Wada A, Yamasaki T, et al. Overexpression of the  
902 *mexC-mexD-oprJ* efflux operon in *nfxB*-type multidrug-resistant strains of *Pseudomonas*  
903 *aeruginosa*. *Mol Microbiol*. 1996;21(4):713-24. Epub 1996/08/01. doi: 10.1046/j.1365-  
904 2958.1996.281397.x. PubMed PMID: 8878035.
- 905 47. Moore RA, DeShazer D, Reckseidler S, Weissman A, Woods DE. Efflux-mediated  
906 aminoglycoside and macrolide resistance in *Burkholderia pseudomallei*. *Antimicrob Agents*  
907 *Chemother*. 1999;43(3):465-70. Epub 1999/02/27. PubMed PMID: 10049252; PubMed  
908 Central PMCID: PMCPMC89145.
- 909 48. Poole K, Tetro K, Zhao Q, Neshat S, Heinrichs DE, Bianco N. Expression of the multidrug  
910 resistance operon *mexA-mexB-oprM* in *Pseudomonas aeruginosa*: *mexR* encodes a  
911 regulator of operon expression. *Antimicrob Agents Chemother*. 1996;40(9):2021-8. Epub  
912 1996/09/01. doi: 10.1128/AAC.40.9.2021. PubMed PMID: 8878574; PubMed Central  
913 PMCID: PMCPMC163466.
- 914 49. Maddocks SE, Oyston PC. Structure and function of the LysR-type transcriptional regulator  
915 (LTTR) family proteins. *Microbiology*. 2008;154(Pt 12):3609-23. Epub 2008/12/03. doi:  
916 10.1099/mic.0.2008/022772-0. PubMed PMID: 19047729.
- 917 50. Hu R-M, Liao S-T, Huang C-C, Huang Y-W, Yang T-C. An inducible fusaric acid tripartite  
918 efflux pump contributes to the fusaric acid resistance in *Stenotrophomonas maltophilia*.  
919 *PLoS ONE*. 2012;7(12):e51053. doi: 10.1371/journal.pone.0051053. PubMed PMID:  
920 23236431; PubMed Central PMCID: PMCPMC3517613.
- 921 51. Nikaido H, Pagès J-M. Broad Specificity Efflux pumps and their role in multidrug resistance  
922 of Gram negative bacteria. *FEMS Microbiol Rev*. 2012;36(2):340-63. doi: 10.1111/j.1574-  
923 6976.2011.00290.x. PubMed PMID: PMC3546547.
- 924 52. Ooi WF, Ong C, Nandi T, Kreisberg JF, Chua HH, Sun G, et al. The condition-dependent  
925 transcriptional landscape of *Burkholderia pseudomallei*. *PLoS Genet*. 2013;9(9):e1003795.  
926 Epub 2013/09/27. doi: 10.1371/journal.pgen.1003795. PubMed PMID: 24068961; PubMed  
927 Central PMCID: PMCPMC3772027.
- 928 53. Mohs A, Silva T, Yoshida T, Amin R, Lukomski S, Inouye M, et al. Mechanism of  
929 stabilization of a bacterial collagen triple helix in the absence of hydroxyproline. *J Biol*  
930 *Chem*. 2007;282(41):29757-65. doi: 10.1074/jbc.M703991200. PubMed PMID: 17693404
- 931 54. Han R, Zwiefka A, Caswell CC, Xu Y, Keene DR, Lukomska E, et al. Assessment of  
932 prokaryotic collagen-like sequences derived from streptococcal Scl1 and Scl2 proteins as a  
933 source of recombinant GXY polymers. *Appl Microbiol Biotechnol*. 2006;72(1):109-15. Epub  
934 2006/03/23. doi: 10.1007/s00253-006-0387-5. PubMed PMID: 16552563.
- 935 55. Leski TA, Caswell CC, Pawlowski M, Klinke DJ, Bujnicki JM, Hart SJ, et al. Identification and  
936 classification of *bcl* genes and proteins of *Bacillus cereus* group organisms and their  
937 application in *Bacillus anthracis* detection and fingerprinting. *Appl Environ Microbiol*.  
938 2009;75(22):7163-72. Epub 2009/09/22. doi: 10.1128/aem.01069-09. PubMed PMID:  
939 19767469; PubMed Central PMCID: PMCPMC2786505.
- 940 56. Sylvestre P, Couture-Tosi E, Mock M. Polymorphism in the collagen-like region of the  
941 *Bacillus anthracis* BclA protein leads to variation in exosporium filament length. *J Bacteriol*.



- 942 2003;185(5):1555-63. Epub 2003/02/20. PubMed PMID: 12591872; PubMed Central  
943 PMCID: PMCPmc148075.
- 944 57. Persikov AV, Ramshaw JAM, Brodsky B. Prediction of collagen stability from amino acid  
945 sequence. *J Biol Chem.* 2005;280(19):19343-9. doi: 10.1074/jbc.M501657200. PubMed  
946 PMID: 15753081.
- 947 58. Gu C, Jenkins SA, Xue Q, Xu Y. Activation of the classical complement pathway by *Bacillus*  
948 *anthracis* is the primary mechanism for spore phagocytosis and involves the spore surface  
949 protein BclA. *J Immunol.* 2012;188(9):4421-31. Epub 2012/03/24. doi:  
950 10.4049/jimmunol.1102092. PubMed PMID: 22442442; PubMed Central PMCID:  
951 PMCPMC3331890.
- 952 59. Herrick S, Blanc-Brude O, Gray A, Laurent G. Fibrinogen. *Int J Biochem Cell Biol.*  
953 1999;31(7):741-6. Epub 1999/09/01. doi: 10.1016/s1357-2725(99)00032-1. PubMed PMID:  
954 10467729.
- 955 60. Vaudaux P, Pittet D, Haeberli A, Huggler E, Nydegger UE, Lew DP, et al. Host factors  
956 selectively increase staphylococcal adherence on inserted catheters: a role for fibronectin  
957 and fibrinogen or fibrin. *J Infect Dis.* 1989;160(5):865-75. Epub 1989/11/01. doi:  
958 10.1093/infdis/160.5.865. PubMed PMID: 2809259.
- 959 61. Ko YP, Flick MJ. Fibrinogen Is at the Interface of Host Defense and Pathogen Virulence in  
960 *Staphylococcus aureus* Infection. *Semin Thromb Hemost.* 2016;42(4):408-21. Epub  
961 2016/04/09. doi: 10.1055/s-0036-1579635. PubMed PMID: 27056151; PubMed Central  
962 PMCID: PMCPMC5514417.
- 963 62. Fitzgerald JR, Loughman A, Keane F, Brennan M, Knobel M, Higgins J, et al. Fibronectin-  
964 binding proteins of *Staphylococcus aureus* mediate activation of human platelets via  
965 fibrinogen and fibronectin bridges to integrin GPIIb/IIIa and IgG binding to the FcγRIIIa  
966 receptor. *Mol Microbiol.* 2006;59(1):212-30. Epub 2005/12/20. doi: 10.1111/j.1365-  
967 2958.2005.04922.x. PubMed PMID: 16359330.
- 968 63. Rhodes KA, Somprasong N, Podnecky NL, Mima T, Chirakul S, Schweizer HP. Molecular  
969 determinants of *Burkholderia pseudomallei* BpeEF-OprC efflux pump expression.  
970 *Microbiology.* 2018;164(9):1156-67. Epub 2018/07/20. doi: 10.1099/mic.0.000691. PubMed  
971 PMID: 30024368; PubMed Central PMCID: PMCPMC6230764.
- 972 64. Crutcher FK, Liu J, Puckhaber LS, Stipanovic RD, Bell AA, Nichols RL. FUBT, a putative  
973 MFS transporter, promotes secretion of fusaric acid in the cotton pathogen *Fusarium*  
974 *oxysporum f. sp. vasinfectum*. *Microbiology.* 2015;161(Pt 4):875-83. Epub 2015/01/30. doi:  
975 10.1099/mic.0.000043. PubMed PMID: 25627440.
- 976 65. Tornroth-Horsefield S, Gourdon P, Horsefield R, Brive L, Yamamoto N, Mori H, et al. Crystal  
977 structure of AcrB in complex with a single transmembrane subunit reveals another twist.  
978 *Structure.* 2007;15(12):1663-73. Epub 2007/12/13. doi: 10.1016/j.str.2007.09.023. PubMed  
979 PMID: 18073115.
- 980 66. Delmar JA, Su CC, Yu EW. Bacterial multidrug efflux transporters. *Annu Rev Biophys.*  
981 2014;43:93-117. Epub 2014/04/08. doi: 10.1146/annurev-biophys-051013-022855. PubMed  
982 PMID: 24702006; PubMed Central PMCID: PMCPMC4769028.
- 983 67. Loftin IR, Franke S, Roberts SA, Weichsel A, Heroux A, Montfort WR, et al. A novel copper-  
984 binding fold for the periplasmic copper resistance protein CusF. *Biochemistry.*

- 985 2005;44(31):10533-40. Epub 2005/08/03. doi: 10.1021/bi050827b. PubMed PMID:  
986 16060662.
- 987 68. Loftin IR, Franke S, Blackburn NJ, McEvoy MM. Unusual Cu(I)/Ag(I) coordination of  
988 *Escherichia coli* CusF as revealed by atomic resolution crystallography and X-ray absorption  
989 spectroscopy. *Protein Sci.* 2007;16(10):2287-93. Epub 2007/09/26. doi:  
990 10.1110/ps.073021307. PubMed PMID: 17893365; PubMed Central PMCID:  
991 PMCPMC2204137.
- 992 69. Huang YW, Hu RM, Yang TC. Role of the pcm-tolCsm operon in the multidrug resistance of  
993 *Stenotrophomonas maltophilia*. *J Antimicrob Chemother.* 2013;68(9):1987-93. Epub  
994 2013/05/01. doi: 10.1093/jac/dkt148. PubMed PMID: 23629016.
- 995 70. Quecine MC, Kidarsa TA, Goebel NC, Shaffer BT, Henkels MD, Zabriskie TM, et al. An  
996 interspecies signaling system mediated by fusaric acid has parallel effects on antifungal  
997 metabolite production by *Pseudomonas protegens* strain Pf-5 and antibiosis of *Fusarium*  
998 *spp.* *Appl Environ Microbiol.* 2015;82(5):1372-82. Epub 2015/12/15. doi:  
999 10.1128/AEM.02574-15. PubMed PMID: 26655755; PubMed Central PMCID:  
1000 PMCPMC4771327.
- 1001 71. Tung TT, Jakobsen TH, Dao TT, Fuglsang AT, Givskov M, Christensen SB, et al. Fusaric  
1002 acid and analogues as Gram-negative bacterial quorum sensing inhibitors. *European J Med*  
1003 *Chem.* 2017;126:1011-20. doi: <https://doi.org/10.1016/j.ejmech.2016.11.044>.
- 1004 72. Ruiz J, M Bernar E, Jung K. Production of siderophores increases resistance to fusaric acid  
1005 in *Pseudomonas protegens* Pf-52015. e0117040 p.
- 1006 73. van Rij ET, Girard G, Lugtenberg BJJ, Bloemberg GV. Influence of fusaric acid on  
1007 phenazine-1-carboxamide synthesis and gene expression of *Pseudomonas chlororaphis*  
1008 strain PCL1391. *Microbiology.* 2005;151(Pt 8):2805-14. Epub 2005/08/05. doi:  
1009 10.1099/mic.0.28063-0. PubMed PMID: 16079356.
- 1010

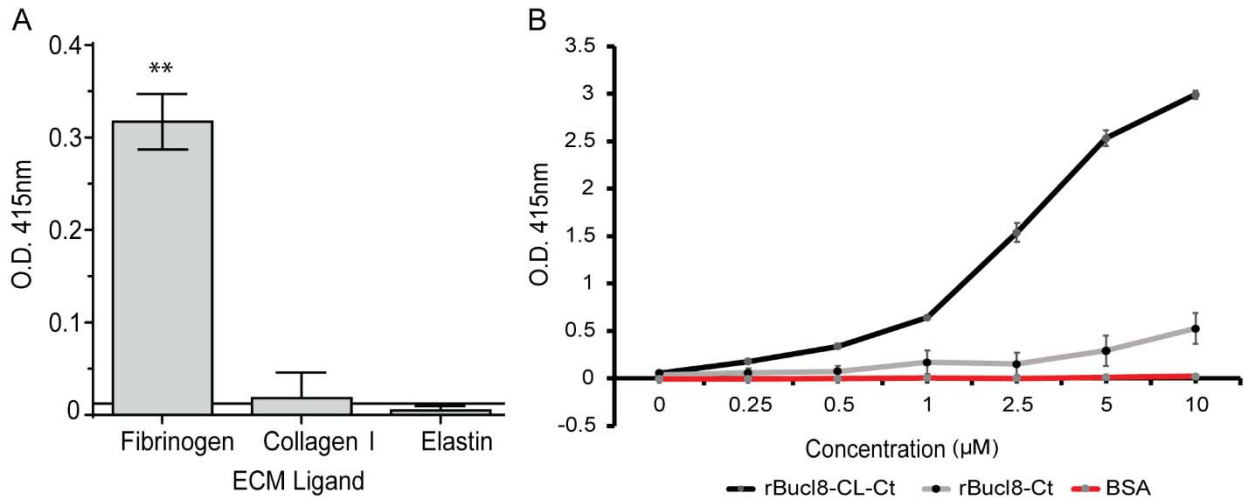


1011

1012 **Fig 1. Structure analysis of extracellular component of the Bucl8 outer membrane**  
 1013 **protein.**

1014 (A) Schematic organization of Bucl8 domain, including signal sequence (SS), outer  
 1015 membrane efflux protein domains 1 and 2 (OEP1, OEP2), collagen-like region (CL) and  
 1016 the C-terminus (Ct). (B) Structural modeling of Bucl8 extracellular region. Model depicts  
 1017 a homotrimeric polypeptide consisting of triple-helical CL domain of rBucl8-CL-Ct and  
 1018 unstructured C-terminus (rBucl8-Ct). The stick model in the inset depicts the triple  
 1019 helical fold of repeating (GAS)<sub>n</sub> collagen sequence of Bucl8-CL. (C) 4-20% SDS-PAGE  
 1020 analysis of recombinant Bucl8-derived constructs. rBucl8-CL-Ct and rBucl8-Ct

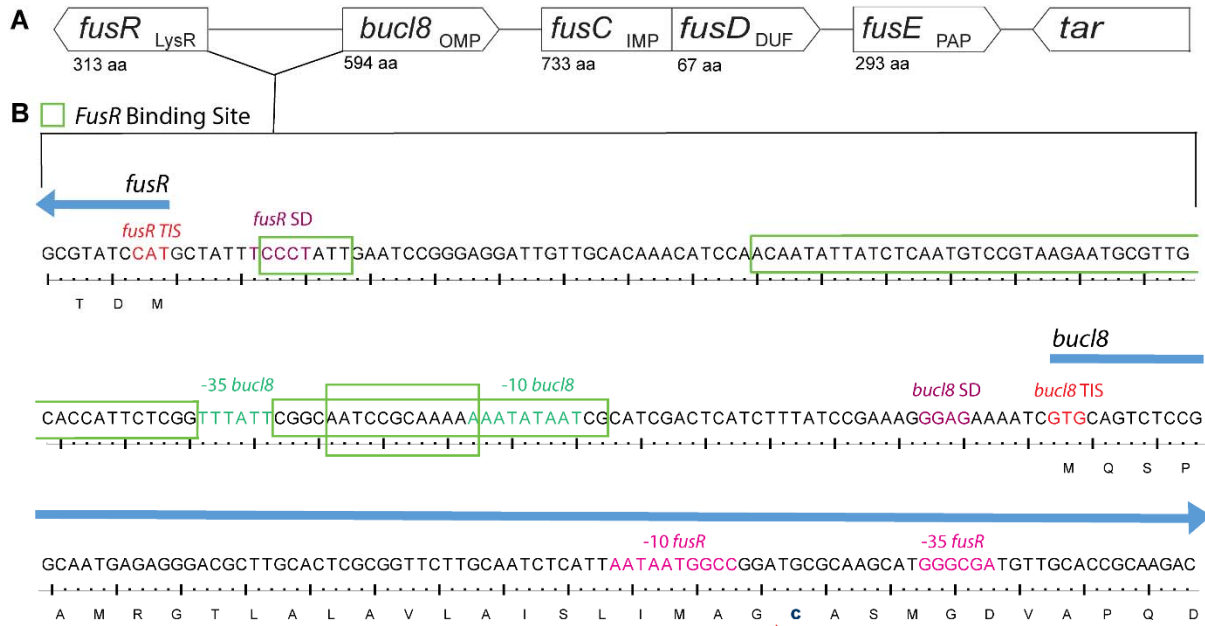
1021 polypeptides were expressed in *E. coli* and purified via His-tag affinity chromatography.  
1022 (D) Circular dichroism (CD) spectroscopy. (upper plot) Wavelength scans of rBucl8-CL-  
1023 Ct were performed at 25°C (solid line) and 50°C (dashed line). A drop in molar ellipticity  
1024 maximum at 220 nm ( $\Theta_{220}$ ) is observed in the CD spectra, indicating the transition from  
1025 triple-helical (25°C) to unfolded form (50°C). (bottom plot) CD spectrum of rBucl8-Ct at  
1026 25°C indicates an unstructured form.



1027  
1028

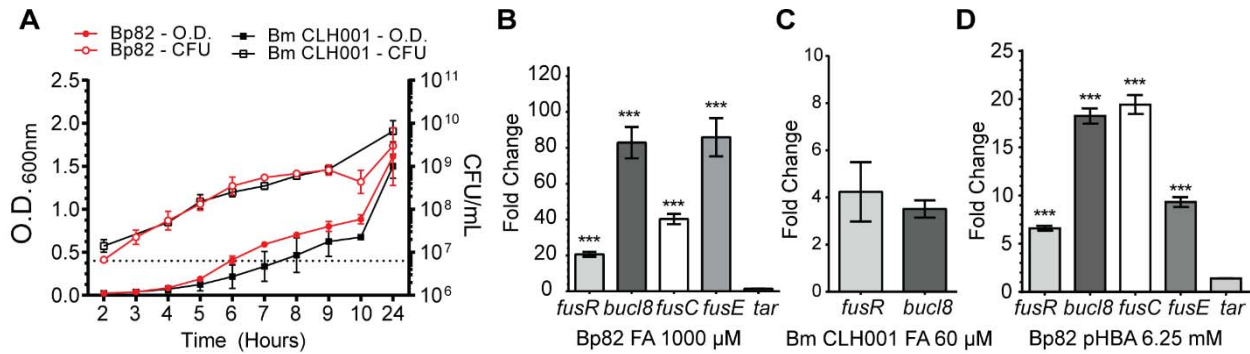
**Fig 2. Binding of rBucl8-derived constructs to extracellular matrix proteins.**

1029 (A) Screening assay for rBucl8-CL-Ct binding to extracellular matrix proteins. Ligand  
1030 binding was tested by ELISA; representative examples of rBucl8-CL-Ct-binding-positive  
1031 and binding-negative ligands are shown. rBucl8-CL-Ct binding was compared  
1032 statistically with binding to BSA-coated wells plus two standard deviations; Student's *t*-  
1033 test,  $**p \leq 0.01$ . (B) Concentration-dependent binding of rBucl8-CL-Ct and rBucl8-Ct to  
1034 fibrinogen. Wells were coated with fibrinogen and either recombinant Bucl8-derived  
1035 protein was added at increasing concentrations. Data represents the mean  $\pm$ SEM of  
1036 three independent experiments ( $n=3$ ), each performed in triplicate wells. Binding was  
1037 detected with an anti-His-tag mAb.



1038  
1039 **Fig 3. Chromosomal locus surrounding *bucl8* gene in *B. pseudomallei* and *B.***  
1040 ***mallei*.**

1041 (A) Schematic of *bucl8*-associated locus with presumed protein function (subscript)  
1042 and amino acid length (aa). Upstream of *bucl8* is gene *fusR*, while downstream are  
1043 genes *fusCD* and *fusE*. Flanking the *bucl8* operon is unrelated downstream gene *tar*.  
1044 LysR, LysR-type transcriptional regulator; OMP, Outer membrane protein; IMP, Inner  
1045 membrane protein; DUF, Domain of unknown function; and PAP, periplasmic adaptor  
1046 protein. (B) Regulatory intergenic region between *fusR* and *bucl8*. Both nucleotide and  
1047 translated sequence are shown. Red arrow indicates cleavage site between the signal  
1048 peptide and N-terminal cysteine linker (bolded).

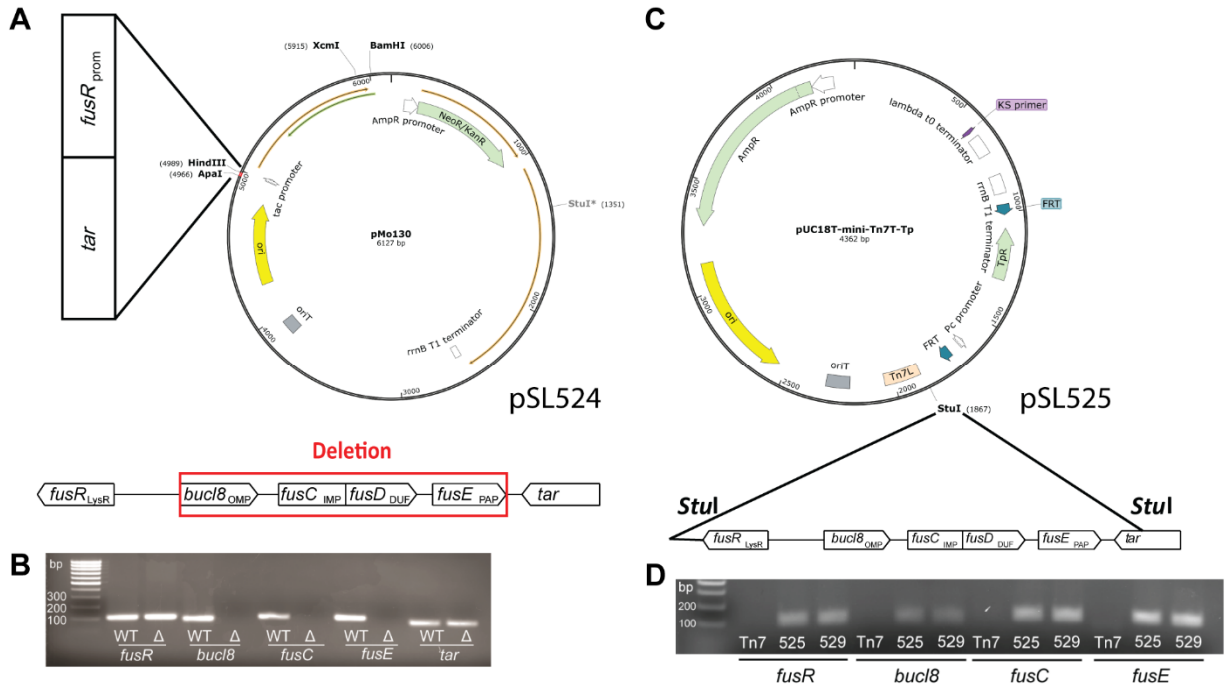


1049

1050 **Fig 4. Effect of FA and pHBA on gene transcription within *fusR-bucl8-fusCD-fusE***  
1051 **operon.**

1052 (A) Growth curves of *B. pseudomallei* strain Bp82 and *B. mallei* strain CLH001.  
1053 Cultures were grown in strain-specific broth and optical density (O.D.) and colony  
1054 forming units (CFU) were recorded. Dotted line represents OD of 0.4. Error bars  
1055 represent  $\pm$ SEM. (B-D) RT-qPCR was performed on RNA samples isolated from  
1056 cultures of the indicated strain, untreated and treated with substrate, at an OD<sub>600</sub> of ~0.4  
1057 for 1 hour. Graph shows fold change of relative gene expression compared to untreated  
1058 cultures and normalized to transcription of 16S rRNA gene. Technical and experimental  
1059 replicates were done in triplicate. One-way ANOVA with Tukey's multiple comparison  
1060 test of the log<sub>10</sub>-transformed fold change. Significance shown is in comparison to *tar*;  
1061 \*\*\* $p < 0.001$ . Error bars represent  $\pm$ SEM. (B) Transcription activation of *fusR-bucl8-*  
1062 *fusCD-fusE* genes in Bp82 with 1000  $\mu$ M FA. The downstream *tar* gene is assumed  
1063 outside of the *fusR-bucl8* operon. (C) Transcription activation of *fusR* and *bucl8* in  
1064 CLH001 with 60  $\mu$ M FA. (D) Transcription activation of Bucl8 regulon in Bp82 with 6.25  
1065 mM pHBA.



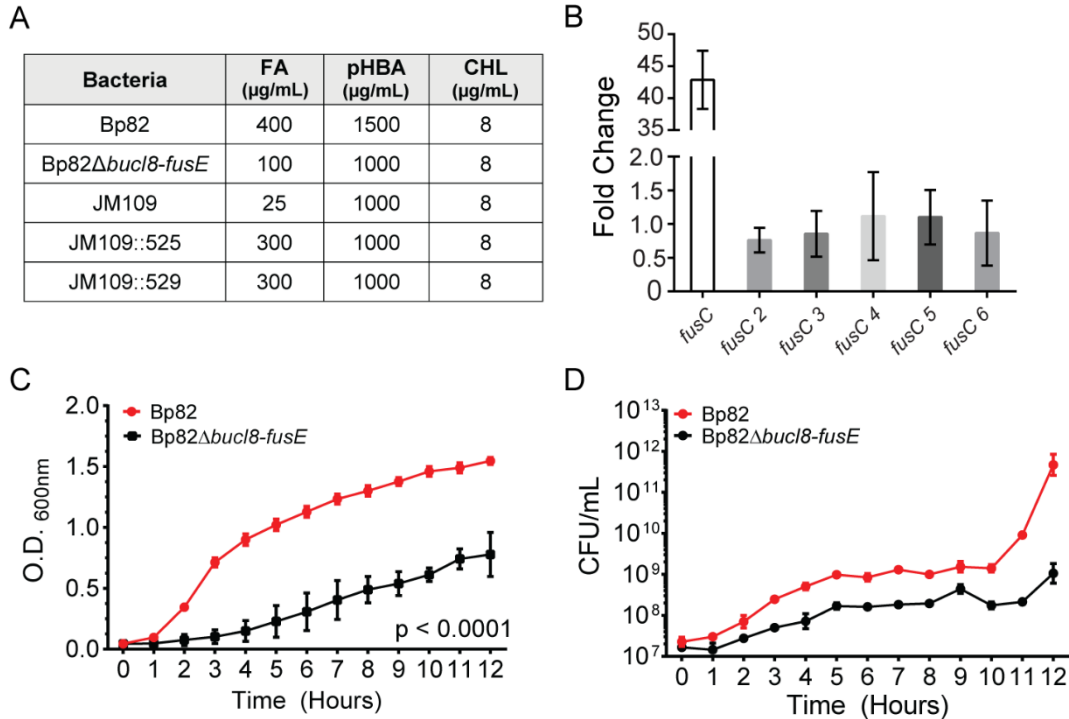


1066  
1067 **Fig 5. Construction of an unmarked *Bucl8*-pump deletion mutant and cloning into**  
1068 **a heterogenous host.**

1069 (A) Strategy for generating an unmarked *Bucl8*-pump deletion mutant. Construction  
1070 of the suicide plasmid construct pSL524. Vector pMo130, which is suicide in  
1071 *Burkholderia*, was used to generate pSL524 plasmid construct for mutagenesis. *HindIII*  
1072 and *ApaI* sites were utilized to clone flanking regions containing *fusR* and *tar* sequences  
1073 to delete the *bucI8-fusE* coding region, depicted below. (B) Analysis of the *bucI8-fusE*  
1074 deletion mutant of Bp82 by PCR. The presence of *bucI8-fusE* genes was tested in the  
1075 genomic DNA isolated from wild type Bp82 (WT) and Bp82 *bucI8-fusE* mutant ( $\Delta$ ). (C)  
1076 Cloning of the *Bucl8*-pump locus for *in-trans* complementation in *E. coli*. Vector  
1077 pUCT18T-mini-Tn7T-Tp was used for cloning of an 8.2-kb genomic Bp82 fragment,  
1078 flanked by *StuI* sites, encompassing *bucI8* locus. (D) Characterization of the pSL525  
1079 and pSL529 constructs. The presence of *fusR-fusE* genes on pSL525 and pSL529



1080 plasmids was tested by PCR. PCR products shown in B and D were analyzed on 1.3%  
1081 agarose gel.



1082

1083 **Fig 6. Analysis of loss-of-function and gain-of-function associated with**  
 1084 **chromosomal deletion and *in-trans* complementation of *BucI8*-pump**  
 1085 **components.**

1086 (A) Changes in sensitivity/resistance patterns in bacterial strains. MIC was  
 1087 determined by plating bacteria on LA containing each substrate. FA, fusaric acid; pHBA,  
 1088 para-hydroxybenzoic acid; CHL, chloramphenicol. (B) Relative expression of *fusC*  
 1089 genes. RT-qPCR was performed on total mRNA isolated from non-treated and FA-  
 1090 treated (1000 µM, 1 hour) Bp82 cultures (OD<sub>600</sub> ~0.4). Graph shows fold change of  
 1091 relative gene expression compared to untreated cultures and normalized to 16S rRNA.  
 1092 Technical and experimental replicates were done in triplicate. (C-D) Effect of  
 1093 chromosomal deletion on growth. Parental strain Bp82 and its *bucI8-fusE* deletion  
 1094 mutant (Bp82Δ*bucI8-fusE*) were grown in LBM broth at 37°C with shaking. Changes in

1095 OD<sub>600</sub> (C) were recorded and CFU numbers (D) by plating on LA medium every hour.  
1096 Data represents the average of three biological replicates. 2-way ANOVA with Tukey  
1097 multiple comparison test, \*\*\*p < 0.001. Error bars represent ±SEM.